Supporting Information for

A Heavy-Metal Trojan Horse: Enterobactin-Directed Delivery of Platinum(IV) Prodrugs to *Escherichia coli*

Chuchu Guo[1] and Elizabeth M. Nolan[1,*]

[1]Department of Chemistry, Massachusetts Institute of Technology, Cambridge, MA 02139

*Corresponding author: lnolan@mit.edu

Phone: 617-452-2495

This supporting information includes:

Supporting Experimental Section

Instrumentation

High-performance liquid chromatography (HPLC). Semi-preparative and analytical HPLC were performed by using an Agilent 1200 series HPLC system outfitted with an Agilent Zorbax reverse-phase C18 column (5 μm, 9.4 × 250 mm) at a flow rate of 4 mL/min and a Clipeus reverse-phase C18 column (5 μm, 4.6 × 250 mm; Higgins Analytical, Inc.) at a flow rate of 1 mL/min, respectively. Preparative HPLC was performed by using an Agilent PrepStar system outfitted with a Phenomenex Luna reverse-phase C18 column (10 μm, 21.2 × 250 mm) at a flow rate of 10 mL/min. The multiwavelength detectors were set to read the absorbance at 220, 280, and 316 (catecholate absorption) nm.

Solvent A was Milli-Q water (18.2 MΩ·cm) with trifluoroacetic acid (TFA, purchased from Millipore Sigma) that was filtered through a 0.2-μm bottle-top filter before use. Solvent B was HPLC grade acetonitrile (MeCN, purchased from Millipore Sigma) with TFA. The amount of TFA in each eluent is indicated in the synthetic procedures. Each HPLC method began with a four-minute equilibration at 0% B followed by a gradient of increasing %B. For analytical HPLC performed to evaluate conjugate purity, the entire portion of each HPLC-purified compound was dissolved in a mixture of 1:1 H_2O/MeCN and an aliquot was taken for HPLC analysis, and the remaining solution was subsequently frozen and lyophilized to dryness.

Liquid chromatography/mass spectrometry (LC/MS). LC/MS was performed using a nominal mass Agilent 6125B mass spectrometer attached to an Agilent 1260 Infinity LC with an electrospray (ESI) source. High-resolution mass spectrometry was

performed using a high-resolution Agilent 6545 mass spectrometer coupled to an Agilent Infinity 1260 LC system with a Jet Stream ESI source. For all LC/MS analyses, solvent A was 0.1% formic acid/H_2O and solvent B was 0.1% formic acid/MeCN (LC/MS grade MeCN, Millipore Sigma). The samples were analyzed using a solvent gradient of 5–95% B over 6 min with a flow rate of 0.4 mL/min. All LC/MS instruments are housed in the MIT DCIF.

Inductively coupled plasma-mass spectrometry (ICP-MS). Metal analysis was conducted using an Agilent 7900 ICP-MS system in helium mode outfitted with an integrated autosampler housed in the Center for Environmental Health Sciences (CEHS) Bioanalytical Core Facility at MIT. To quantify Fe concentration, the instrument was calibrated using standards prepared by serial dilution of an environmental calibration standard solution (1000 ppm each of Ca, Fe, K, Mg, Na; 10 ppm each of Ag, Al, As, Ba, Be, Cd, Co, Cr, Cu, Mn, Mo, Ni, Pb, Sb, Se, Th, Tl, U, V, Zn; Agilent, part number 5183-4688). To quantify Pt concentration, the instrument was calibrated using standards prepared by serial dilution of a Pt standard solution (1 ppm Pt; Millipore Sigma). Terbium (1 ppb Tb; Agilent) was used as an internal standard. All samples were prepared as 2 mL solutions in 5% HNO_3 (Honeywell, TraceSELECT; 69.0%) in 15 mL Falcon tubes, transferred to ICP-MS polypropylene vials (Agilent) and analyzed.

For whole-cell metal analyses of bacterial cells or HEK293T cells, cell pellets diluted into solutions of 3% HNO_3 were liquefied using a Milestone UltraWAVE digestion system housed in the CEHS Core Facility at MIT. A standard microwave protocol (15 min ramp to 200 °C at 1,500 W power; 10 min ramp to 220 °C at 1,500 W power) was used for the acid digestion.

NMR spectroscopy. ^{1}H NMR spectra were collected on a two-channel Bruker Avance-III HD Nanobay 400 MHz spectrometer or a three-channel Bruker Avance Neo 500 MHz spectrometer (both are equipped with a 5-mm liquid-nitrogen cooled Prodigy broad band observe cryoprobe). ^{195}Pt NMR and 2-dimentional (2-D) NMR spectra were collected on a three-channel Bruker Avance Neo 500 MHz spectrometer (equipped with a 5-mm BBFO SmartProbe) at ambient probe temperature (293 K). All NMR spectrometers are housed in the MIT Department of Chemistry Instrumentation Facility (DCIF).

Optical absorption spectroscopy. Optical absorption spectra were recorded on a Beckman Coulter DU800 spectrophotometer (1-cm quartz cuvettes, Starna).

Microscopy. Phase-contrast and fluorescence microscopy imaging were carried out using a Zeiss Axioplan2 upright microscope equipped with a 100× oil-immersion objective lens. Phase-contrast images were acquired using the trans phase channel. For LIVE/DEAD cell viability assays, the Texas Red (λ_{ex} = 532–587 nm; λ_{em} = 608–683 nm) and GFP (λ_{ex} = 457–487 nm; λ_{em} = 502–538 nm) channels were used to acquire images of the DEAD (red) and LIVE (green) cells, respectively.

Synthesis

General synthetic methods. Anhydrous *N,N*-dimethylformamide (DMF) and dichloromethane (DCM) were purchased from VWR. Anhydrous dimethyl sulfoxide (DMSO) was purchased from Millipore Sigma and used as received. All other chemicals were purchased from Millipore Sigma, VWR or Alfa Aesar in the highest available purity and used as received.

EMD TLC silica gel 60 F_{254} plates were used for analytical thin layer chromatography. EMD PLC silica gel 60 F_{254} plates of 2-mm thickness were used for preparative TLC. Sigma-Aldrich silica gel (70–230 mesh, 60 Å) was used for flash column chromatography.

Syntheses of Ent **1**, L-Ent-N_3 **7** and D-Ent-N_3 and *cis, cis, trans*-$[Pt(NH_3)_2Cl_2(OOCCH_3)(OH)]$ were based on published procedures.[1-4]

***cis, cis, trans*-[$Pt(NH_3)_2Cl_2(OOCCH_3)(OOCCH_2CH_2C{\equiv}CH)$] (denoted hereafter as Pt(IV)-alkyne 6).** The synthesis of Pt(IV)-alkyne was performed using a literature procedure with modifications.[5] *cis, cis, trans*-$[Pt(NH_3)_2(Cl)_2(OOCCH_3)(OH)]$ (50 mg, 0.13 mmol) was suspended in anhydrous DMF (6 mL). 4-Pentynoic acid (53 mg, 0.053 mmol) was dissolved in anhydrous DMF (1.3 mL) and combined with *N,N'*-dicyclohexylcarbodiimide (DCC, 115 mg, 0.56 mmol). The mixture was placed in an ultrasonic bath for 15 min, during which time a white precipitate formed. The mixture was centrifuged (4,500 rpm, 15 min, room temperature), and the supernatant was added slowly to the above suspension. The reaction was purged with N_2 and stirred in the dark at room temperature for 16 h, resulting in a clear yellow solution. The reaction mixture was concentrated by air stream to yield a yellow oil, to which water (12 mL) was added. The mixture was sonicated for 5 min, which resulted in precipitation of the dicyclohexylurea byproduct, which was removed by vacuum filtration. The filtrate was washed with Et_2O and the combined solution was lyophilized, affording a yellow powder. The crude product was dissolved in 1:1 H_2O/MeCN, filtered through a 0.45-μm PTFE filter (purchased from VWR), and purified by preparative HPLC (0–100% B over 30 min, 10 mL/min, 0.1% TFA in solvents A and B). The eluate at 15.4 min was collected and

lyophilized to give the pure product as a white powder (33 mg, 56% yield). MS (ESI+): $[M+H]^+$ *m/z* calcd, 457.0038; found, 457.0016. $[M+Na]^+$ *m/z* calcd, 478.9857; found, 478.9843. ^{1}H NMR (500 MHz, D_2O): δ 2.04 (3H, s), 2.40 (1H, t, J = 2.6 Hz), 2.38–2.39 (2H, m), 2.57–2.60 (2H, t, J = 7.0 Hz). ^{195}Pt NMR (500 MHz, D_2O): δ 1073.82.

L-Ent-Pt(IV) (L-EP, 4). L-Ent-N_3 **1** (38.3 mg, 0.042 mmol) was dissolved in DMF (600 μL) to give a 70 mM solution. The solution was divided into aliquots (9.5 μL, 0.7 mg in each aliquot). Pt(IV)-alkyne **6** (48 mg, 0.10 mmol) was dissolved in DMF (179 μL) to give a 586 mM solution. To each aliquot of the L-Ent-N_3 **7** solution (70 mM)**,** 2.8 μL of the Pt(IV)-alkyne **6** solution (586 mM) was added, followed by 8 μL of Milli-Q water. A DMF solution containing 50 mM *tris*[(1-benzyl-1*H*-1,2,3-triazol-4-yl)methyl]amine (TBTA) and 50 mM $Cu(MeCN)_4PF_6$ was freshly prepared and 19.7 μL of the solution was added to each aliquot. The resulting solutions were briefly mixed by using a vortex mixer and incubated on a benchtop rotator at room temperature in the dark. After 3 h, each aliquot was diluted with 160 μL of 1:1 H_2O/MeCN, centrifuged (13,000 rpm, 10 min, 4 °C), and purified by preparative HPLC (0–100% B over 30 min, 10 mL/min, 0.005% TFA was used in solvent A and B; this low TFA % was used to prevent decomposition). The product eluted at 20.9 min, and the collected fractions were combined and lyophilized, which afforded a pale-green powder. Further purification was performed by semi-preparative HPLC (0–100% B over 30 min, 4 mL/min, 0.005% TFA). The product eluted at 13.8 min and was collected and lyophilized, which afforded L-EP as a white powder (3.7 mg, 6%). The product purity was evaluated by analytical HPLC (0–100% B over 30 min, 1 mL/min, 0.005% TFA; retention time 17.3 min). HRMS (ESI+): $[M+H]^+$ *m/z* calcd, 1370.2569; found, 1370.2650. $[M+Na]^+$ *m/z* calcd, 1391.2407; found, 1391.2474. ^{1}H NMR (500 MHz,

DMSO_d_6): δ 1.92 (3H, s), 2.53 (2H, t, J = 7.6 Hz), 2.81 (2H, t, J = 7.3 Hz), 3.52 (12H, m), 3.80 (2H, t, J = 5.4), 4.3–4.45 (5H, m), 4.63–4.69 (3H, m), 4.89–4.96 (3H, m), 6.56 (6H, br), 6.75 (2H, t, J = 8.0 Hz), 6.98 (2H, d, J = 7.8 Hz), 7.36 (2H, d, J = 8.2 Hz), 7.46 (1H, m), 7.86 (1H, s), 7.93 (1H, m), 8.32 (1H, t, J = 5.5 Hz), 9.12 (2H, d, J = 6.8 Hz), 9.29 (1H, d, J = 7.0 Hz), 9.41 (2H, s), 9.72 (1H, s), 11.62 (2H, s), 11.92 (1H, s). ^{195}Pt signal was detected by ^{1}H-^{195}Pt HMQC NMR (500 MHz, DMSO_d_6): δ 1226.95 (s). The product structure was also characterized by 2-dimensinal (2-D) NMR including ^{1}H-^{1}H COSY, ^{1}H-^{13}C HSQC and ^{1}H-^{13}C HMBC.

D-Ent-Pt(IV) (D-EP, 5). D-Ent-Pt(IV) was synthesized as described for L-Ent-Pt(IV) (L-EP, **4**) except that D-Ent-N_3 was employed instead of L-Ent-N_3. HRMS (ESI+): $[M+H]^+$ *m/z* calcd, 1370.2569; found, 1370.2669. $[M+Na]^+$ *m/z* calcd, 1391.2407; found, 1391.2459. ^{1}H NMR (500 MHz, DMSO_d_6): δ 1.92 (3H, s), 2.53 (2H, t, J = 7.6 Hz), 2.81 (2H, t, J = 7.3 Hz), 3.52 (12H, m), 3.80 (2H, t, J = 5.4), 4.38–4.45 (5H, m), 4.63–4.69 (3H, m), 4.89–4.96 (3H, m), 6.56 (6H, br), 6.75 (2H, t, J = 8.0 Hz), 6.98 (2H, d, J = 7.8 Hz), 7.36 (2H, d, J = 8.2 Hz), 7.46 (1H, s), 7.86 (1H, s), 7.93 (1H, s), 8.33 (1H, t, J = 5.5 Hz), 9.12 (2H, d, J = 6.8 Hz), 9.29 (1H, d, J = 7.0 Hz), 9.41 (2H, s), 9.73 (1H, s), 11.62 (2H, s), 11.92 (1H, s). ^{195}Pt signal was detected by ^{1}H-^{195}Pt HMQC NMR (500 MHz, DMSO_d_6): δ 1226.95 (s). The product structure was also characterized by 2-dimensinal (2-D) NMR including ^{1}H-^{1}H COSY, ^{1}H-^{13}C HSQC and ^{1}H-^{13}C HMBC.

Storage and handling of Ent and Ent-Pt(IV) conjugates

All precursors, Ent and Ent-Pt(IV) conjugates were stored as either powders or DMSO stock solutions at -20 °C. The concentration of Ent stock solutions (~10 mM) were

determined by using Beer's law and the reported extinction coefficient for enterobactin in MeOH (ε_{316} = 9500 M^{-1} cm^{-1}).[6] An aliquot of the DMSO stock solution was diluted into MeOH for this analysis. Concentrations of L-EP and D-EP stock solutions were determined by quantifying Pt concentration using ICP-MS. The stock solution concentrations were 5–12 mM. To minimize multiple freeze–thaw cycles, the stock solutions were divided into 10 μL aliquots and stored at -20 °C. Aliquots were routinely analyzed by analytical HPLC to confirm the integrity of the samples.

Stability evaluation of L-Ent-Pt(IV)

A 0.5-μL aliquot of a DMSO stock solution of L-EP (5.2 mM determined by ICP-MS) was diluted in 250 μL of water, phosphate buffered saline (PBS), or modified M9 medium with varying thiamine concentrations. The resulting mixtures were divided into five 50-μL aliquots. The aliquots were incubated at 30 °C with shaking at 150 rpm in the dark for 0, 2, 5, 10 and 20 h, respectively. Aliquots were flash frozen in liquid N_2 at each time point and stored at -80°C before HPLC analysis. HPLC samples were prepared thawing each sample and centrifuging at 13,000 rpm for 10 min, and the resulting supernatants were analyzed by analytical HPLC (0–100 B% in 30 min, 1 mL/min, 0.005%TFA in solvents A and B). The percent of remaining L-EP at each time point was determined by integrating the peak area of L-EP (17.3 min) in each sample. The peak areas were normalized to that of the sample at t = 0 min. The correlation of peak area versus time was plotted, and the half-life ($t_{1/2}$) was estimated from each curve. Decomposition products were analyzed by LC/MS. This experiment was performed once for optimizing growth medium conditions.

Microbiology, microscopy, and cell culture methods

General materials. Lysogeny broth (LB; tryptone 10 g/L, yeast extract 5 g/L, NaCl 10 g/L), M9 minimal salts 5×, casamino acids, and agar were purchased from Becton Dickinson (BD). LB medium and Milli-Q water (18.2 MΩ·cm, 0.22-μm filter) used for bacterial cultures or for preparing working solutions of the tested compounds were sterilized in an autoclave. Modified M9 medium was sterilized by passage through a sterile 0.22-μm filter. Sterile polypropylene culture tubes and adhesive PCR film seals were purchased from VWR. Sterile polystyrene 96-well plates and 9-well plates used for culturing were purchased from Corning Incorporated. LIVE/DEAD BacLight Bacterial Viability Kits were purchased from Thermo Fisher (Invitrogen Molecular Probes). Agarose (PCR grade) for microscopy was purchased from Bio-Rad. Microscope slides and microscope cover glasses were purchased from VWR. Cisplatin (≥99.9% trace metals basis) and $Fe(acac)_3$ (≥99.9% trace metals basis) were purchased from Sigma-Aldrich.

Bacterial strains. Bacterial strains employed in this study are summarized in **Table S1.** Freezer stocks were prepared from single colonies in 25% glycerol/ LB medium.

General procedures for bacterial growth assays and microscopy. Growth of *E. coli* under Fe-deficient conditions was performed in a modified M9 medium (Na_2HPO_4 6.8 g/L, KH_2PO_4 3 g/L, NaCl 0.5 g/L, NH_4Cl 1 g/L, 0.4% glucose, 0.2% casein amino acids, 2 mM $MgSO_4$, 0.1 mM $CaCl_2$, 0.6 μg/mL thiamine). The Fe content of modified M9 medium was determined by ICP-MS to be 0.6–0.7 μM Fe. These Fe-deficient conditions cause *E. coli* to express siderophore biosynthesis and transport machinery, including genes for enterobactin biosynthesis and transport encoded by the enterobactin gene cluster as well as the *iroA* cluster for salmochelin biosynthesis and transport.

Working solutions of Ent-Pt(IV) and Pt(IV)-alkyne were prepared via dilutions in 10% DMSO/H_2O. Working solutions of cisplatin were freshly prepared by dissolving cisplatin in modified M9 medium before treatment. The Fe(III)-bound L-EP and D-EP complexes were prepared prior to all microbiology and imaging assays because the modified M9 medium contains insufficient Fe to fully complex the siderophore following addition to the culture. $Fe(acac)_3$ (25 mM stock in DMSO, concentration determined by ICP-MS) was used to prepare the Fe(III) complexes, which were formed by incubating 10 μL of L-EP and D-EP working solution with 0.9 μL of a 10× $Fe(acac)_3$ solution in 10% DMSO/H_2O for 5 min prior to addition to the culture. We note that L-EP and D-EP refer to the corresponding ferric complexes in the discussion of the biological assays. For all microbiology assays, the final cultures contained 1% v/v DMSO, except for cultures with cisplatin treatment which do not contain DMSO.

Overnight cultures of *E. coli* were prepared in 15 mL polypropylene tubes by inoculating 5 mL of medium with the appropriate freezer stock. The overnight cultures were incubated at 37 °C for 16–18 h in a tabletop incubator set at 150 rpm. Each overnight culture was diluted 1:100 into 5 mL of fresh medium at 37 °C with shaking at 150 rpm until OD_{600} reached 0.6 ± 0.1 (measured on a Beckmann Coulter DU800 spectrophotometer). Each culture was subsequently diluted in fresh medium to achieve an OD_{600} value of 0.005 (~5 × 10^6 CFU/mL). A 90 μL aliquot of the diluted culture was combined with a 10 μL aliquot of a 10× working solution of in a 96-well plate. The plate was sealed with an adhesive film (purchased from VWR) and incubated at 30 °C with shaking at 500 rpm for 20 h in the BioTek LogPhase 600 (LP600) microbiology reader (96-well plate format). Growth curves were recorded as OD_{600} values that were collected

every hour in the LP600 microbiology reader. Growth assays of L-EP were performed using a two-fold dilution series spanning 0–60 μM, and assays of D-EP were performed using a ten-fold dilution series spanning 0–10 μM. Each well condition was prepared in duplicate and at least five independent replicates using two synthetic batches of each conjugate and were performed on different days. The resulting mean OD_{600} values are reported, and the error bars are the standard deviation from the independent replicates. Statistical differences compared to untreated controls were calculated using two-tailed student *t* test assuming unequal variances.

Samples for microscopy were prepared by taking aliquots of *E. coli* culture at t = 11 h (mid-log phase). For samples that require only phase-contrast imaging, a 5 μL aliquot of each culture was pipetted on an agarose pad (1% w/w agarose/Milli-Q water) which was placed on a microscope slide. The sample was then covered with a glass coverslip. For LIVE/DEAD viability assays, a 90 μL aliquot of each bacterial culture was centrifuged at 3,000 rpm at 4 °C for 15 min. The resulting cell pellet was resuspended in 0.85% NaCl and the OD_{600} was adjusted to 0.2 using 0.85% NaCl. A 25 μL aliquot of each bacterial suspension was incubated with 25 μL of LIVE/DEAD dye mixture (48 μM SYTO9 and 240 μM propidium iodide) at 30 °C for 15 min in the dark, and 5 μL of the suspension was pipetted on an agarose pad which was placed on a microscope slide. The sample was then covered with a glass coverslip. For each type of microscopy experiment, each condition was repeated in at least three biological replicates using two different synthetic batches. Representative micrographs for each condition are shown in figures.

We selected 11 h as the time point to determine inhibitory effects and morphological changes because of the following considerations: (i) the 11 h time point is

in the mid-log phase of bacterial growth as determined by growth curves; (ii) there is sufficient cell density to determine growth inhibitory effects and have sufficient cells to image; (iii) initial microbiology studies indicated that the stability of L-EP under these conditions was sufficient for our studies (*vide infra*).

We note that the OD_{600} values may be affected by bacterial filamentation with filamentation causing enhanced OD_{600} relative to a culture of the same cell density exhibiting normal morphology. Consequently, we believe the microscopy studies are more revealing in terms of L/D-EP activity.

Image analysis. The microscopy images were processed using the FIJI software (8-bit image type). For phase-contrast images, contrast enhancement was performed by setting saturated pixels as 0.1%. For fluorescence images, fluorescence background subtraction was performed using a rolling ball method with a radius of 150 pixels.

For cell counting, samples were prepared and imaged from at least three biological replicates. Images were acquired at three channels (trans-phase, Texas Red and GFP). 500–1000 cells were counted for each condition. Cell size was measured based on phase-contrast images. By adjusting threshold using available algorithms in FIJI, cells were identified as particles in the resulting binary images. The perimeter of each particle was measured by the software. We note that most of normal and elongated cells can be well-identified by algorithms, but the selection of many filamentous cells needs to be adjusted manually using the polygon tool. Cell viability was determined by counting red and green cells manually based on the corresponding fluorescence images.

Induction of lysogenic bacteria. The induction of lysogenic bacteria was performed based on a published procedure.[7] *E. coli* W3104 was inoculated in 5 mL of

modified M9 medium and grown for 18 h at 37 °C. A 50 μL aliquot of the overnight culture was diluted in 5 mL of modified M9 medium, which was then incubated at 37 °C until the OD_{600} reached 0.5 (~7 h). Then, 0.5 μL aliquots of bacterial culture were added to 100 μL portions of modified M9 medium containing 0 (untreated), 7.5, 15 and 30 μM cisplatin in a 96-well plate. After incubation at 30 °C for 10 h, each culture was diluted 1:10, 1:100, and 1:1000, and 10 μL of each diluted culture was spotted onto an LB agar plate on which a lawn of *E. coli* CFT073 had been freshly plated. After spotting, the plate was incubated at 37 °C for 12 h to allow plaque formation. To test the effect of L-EP, 0.5 μL aliquot of exponentially growing *E. coli* W3104 culture was then incubated in 100 μL of the modified M9 medium which contained 15 μM L-EP, 15 μM Ent and 1% DMSO, respectively.

The *E. coli* CFT073 lawn was prepared by inoculating 4 mL of molten top agar (0.5% LB agar) with 100 μL of an overnight culture of *E. coli* CFT073 grown in LB medium. Following gentle mixing, 3 mL of the inoculated molten top agar was layered atop a preheated (37 °C) LB agar plate and allowed to solidify.

Pt uptake by *E. coli*. *E. coli* CFT073 was inoculated in 5 mL of modified M9 medium and grown for 18 h at 37 °C. A 50 μL aliquot of the overnight culture was diluted in 5 mL of modified M9 medium, which was then incubated at 37 °C until the OD_{600} reached 0.6. A 4 mL portion of the culture was centrifuged at 3,500 rpm and 4°C for 10 min, and the resulting cell pellet was resuspended in 1 mL of fresh modified M9 medium. Then, to a 90 μL aliquot of the diluted culture, a 10 μL aliquot working solution of 150 μM L-EP, D-EP, or Pt(IV)-alkyne (in 10% DMSO/H_2O) was added. After incubation at 30 °C with shaking at 150 rpm for 30 min, cell pellets were harvested by centrifuging each

culture at 3,500 rpm for 10 min. To measure the Pt content in the supernatant, 90 μL of each supernatant was diluted into 1.91 mL of 5% HNO_3 for ICP-MS analysis. To measure the cell-associated Pt content, the cell pellets were first washed with fresh modified M9 medium, and then washed with fresh modified M9 containing 2% w/w aqueous EDTA. The resulting cell pellets were suspended in 2 mL of 5% HNO_3 and digested for ICP-MS analysis. Mass of cell-associated Pt and mass of Pt in the supernatant of each sample were calculated using Pt contents determined by ICP-MS. Cell-associated Pt% was determined according to equation 1.

$$\text{Cell-associated Pt\%} = \frac{\text{mass of cell-associated Pt (μg)}}{\text{mass of cell-associated Pt (μg)} + \text{mass of Pt in the supernatant (μg)}} \quad \text{(eq 1)}$$

Pt uptake by HEK293T cells. Materials for tissue culture were kindly provided by the Shoulders lab at MIT. HEK293T cells were purchased from ATCC. The DMEM medium was purchased from Corning Incorporated. Penicillin and streptomycin were purchased from Corning Incorporated.

HEK293T cells (passages 12–18) were plated at a density of 750,000 cells per well in a 6-well plate (2.5 mL/well) in DMEM supplemented with 1% penicillin/streptomycin and incubated at 37 °C and 5% CO_2 for 24 h. Working solutions of L-EP and D-EP (6 μM) were prepared in 10% DMSO/PBS (PBS purchased from Millipore Sigma). Working solutions of cisplatin were freshly prepared by dissolving cisplatin in PBS (6 μM) before treatment. Each working solution (0.5 mL) was added to each well of cell culture to give the final treatment concentration as 1 μM. Cells were treated for 6 h at 37°C and 5% CO_2, transferred to a 15 mL conical tube and centrifuged at 500 rcf for 5 min. To measure the

Pt content in the supernatant, 200 μL of each supernatant was diluted into 1.8 mL of 5% HNO_3 for ICP-MS analysis. To measure the cell-associated Pt content, cell pellets were washed with 2 mL of PBS three times, and the resulting cell pellets were suspended in 2 mL of 5%HNO_3 and digested for ICP-MS analysis. Mass of cell-associated Pt and mass of Pt in the supernatant of each sample were calculated using Pt contents determined by ICP-MS. Cell-associated Pt% were determined by ICP-MS as described above (eq 1).

Supporting Discussion

We examined the stability of L-EP in a modified M9 growth medium supplemented with 16.5 μg/mL of thiamine that we employed in prior studies of Ent–antibiotic conjugates.[8-10] Analytical HPLC revealed that apo L-EP decomposed in this modified M9 medium with a $t_{1/2}$ < 2 h at 30 °C (**Figures S2, S3A**). The HPLC chromatograms showed loss of the L-EP peak at 17.3 min and formation of a new peak at 17.6 min. LC/MS analysis of the new peak afforded a *m/z* of 1012.3 for the major ion species, which corresponds to the Ent-containing axial ligand (theoretical $[M+H]^+$ = 1012.3, **Figure S2** compound **d**). This result indicated that L-EP readily decomposed with the release its two carboxylate axial ligands in the modified M9 medium. Other decomposition peaks included hydrolysis products of the Ent-containing axial ligand where (i) the Ent trilactone moiety was linearized by one ester hydrolysis event (compound **b**) and (ii) further degraded to the linear dimer form by a second ester hydrolysis event (compound **a**). This analysis prompted us to further examine the stability of L-EP. Previous studies of Pt(IV) complexes demonstrated that release of the axial ligand of a Pt(IV) center can result from hydrolysis or reduction.[11-13] Moreover, the Ent trilactone is prone to hydrolysis.[14] Consequently, we considered these three degradation pathways in our subsequent experiments.

Stability in water and PBS: We first tested the stability of L-EP towards hydrolysis by incubating it in water and found that the molecule is stable in water with negligible decomposition observed during the 20-h incubation at 30 °C (**Figure S3B**). We then evaluated the stability of L-EP in the presence of phosphate salts (Na_2HPO_4 and KH_2PO_4), which are components of the modified M9 medium, by incubating it in PBS and found a

$t_{1/2}$ ~ 5 h (**Figure S3C**). Unlike the decomposition pattern we observed for L-EP incubated in the modified M9 medium (**Figure S2**), HPLC and LC/MS revealed that in PBS the Pt(IV) moiety retained its axial ligands over the 20-h incubation, and that the predominant decomposition pathway was the hydrolysis of the Ent moiety (**Figure S4A**). We also evaluated the stability of Ent in PBS, which showed a similar hydrolysis pattern (**Figure S4B, S4C**).

Further analysis of L-EP stability in the modified M9 medium: We then investigated the effect of glucose and casamino acids (medium components) by incubating L-EP in modified M9 medium without added thiamine and found a $t_{1/2}$ ~ 5 h (**Figure S3D**). Under these conditions, the decomposition pathway was similar to that in PBS; the Pt(IV) moiety retained its axial ligands and Ent hydrolysis occurred (HPLC not shown). Consequently, we speculated that thiamine content of the medium could be problematic for L-EP stablity. Thiamine is a cofactor involved in redox chemistry, and we further speculated that the instability of L-EP in the modified M9 medium resulted from redox chemistry and reduction of the Pt(IV) center, which causes release of the two axial ligands.[15]

Because thiamine is required for the growth of *E. coli* CFT073 mutants employed in this study, we decreased the thiamine concentration in the modified M9 medium to 0.6 μg/mL and found that L-EP showed enhanced stability with a $t_{1/2}$ ~ 5 h at 30 °C (**Figure S3E**). Although *E. coli* growth was generally slower with this reduced thiamine level, the majority of strains grew well and reached mid-log phase after ~11 h of growth at 30 °C (**Figures S20–S23**). Initial microbiology studies indicated that the stability of L-EP under these conditions was sufficient in this medium for our studies. In particular, following 11-

h treatment with L-EP, siderophore receptor/transporter-dependent growth inhibitory effects and morphological changes were observed among the *E. coli* strains used in this study. Therefore, we moved forward using modified M9 medium with 0.6 μg/mL of thiamine and determining bacterial growth and morphology after 11-h treatment for all microbiology assays presented in this work.

Potential uptake of L-EP decomposition products. We note that bacterial uptake of L-EP decomposition products identified in the stability study may occur during the assays presented in this work. In particular, uptake of the released axial Ent ligand (**d** in **Figure S2B**) and its hydrolysis products (**a** and **b** in **Figure S2B**) would result in Fe(III) uptake in the absence of Pt uptake and potentially contribute to enhanced bacterial fitness. Uptake of L-EP hydrolysis products that contain the Pt(IV) cargo and a hydrolyzed Ent moiety (**e**, **f**, **g** in **Figure S4A**) may also occur.

Although we did not perform the stability test on D-EP, we expect similar results for its stability in PBS and modified media containing different levels of thiamine.

Supporting Tables

Table S1. Bacterial strains employed in this study.[8, 16]

Strain	Relevant characteristics or genotype	Source / reference
E. coli K12 BW25113	Common lab strain, non-pathogenic	[16]
E. coli K12 *fepA*	Single gene knock-out of *E. coli* K12	[16]
E. coli CFT073	Clinical isolate, UPEC	ATCC 700928
E. coli MSC 206	CFT073 ΔfepA::kan (KanR)	[8]
E. coli MSC 219	CFT073 ΔiroN::tetRA (TetR)	[8]
E. coli MSC 228	CFT073 ΔfepC::kan (KanR)	[8]
E. coli MSC 230	CFT073 ΔfepDG::kan (KanR)	[8]
E. coli MSC 216	CFT073 ΔfepA::kan ΔiroN::tetRA (KanR TetR)	[8]
E. coli W3104	Lysogenic for coliphage lambda	Carolina Biological

Table S2. Quantitative analysis of L-EP-induced bacterial morphologies and viability.

Strain	[L-EP] (μM)	Normal size (%)	Elongation (%)	Filamentation (%)	Extreme filamentation (%)	Viability (%)
E. coli CFT073	0	99.7	0.3	0.0	0.0	96.7
	7.5	77.7	18.2	3.9	0.2	88.1
	15	73.2	18.8	7.0	1.1	80.1
	30	60.5	22.4	13.0	4.1	75.7
	60	31.4	29.3	21.1	18.2	52.9
E. coli CFT073 *fepC*	0	100.0	0.0	0.0	0.0	98.7
	7.5	99.3	0.7	0.0	0.0	99.3
	15	96.6	3.4	0.0	0.0	99.6
	30	93.7	6.3	0.0	0.0	97.1
	60	78.7	18.4	2.8	0.0	97.0
E. coli CFT073 *fepDG*	0	99.7	0.3	0.0	0.0	99.4
	7.5	97.7	2.1	0.2	0.0	98.8
	15	97.2	2.8	0.0	0.0	97.5
	30	91.9	8.1	0.0	0.0	98.5
	60	82.8	15.2	1.9	0.1	95.4
E. coli CFT073 *fes*	0	100.0	0.0	0.0	0.0	98.8
	7.5	69.1	21.2	8.7	1.0	42.2
	15	48.6	18.7	15.8	16.9	66.2
	30	63.1	12.2	9.9	14.8	66.2
	60	39.3	16.4	18.0	26.3	41.2
E. coli CFT073 *iroD*	0	100.0	0.0	0.0	0.0	97.7
	7.5	60.6	30.8	7.9	0.7	77.2
	15	55.0	27.4	15.3	2.3	70.6
	30	42.8	27.2	19.0	11.0	60.7
	60	48.1	17.8	14.8	19.3	59.0
E. coli K12	0	100.0	0.0	0.0	0.0	96.0
	7.5	54.4	20.4	14.8	10.3	68.2
	15	30.5	24.9	13.8	30.8	57.6
	30	38.1	10.1	14.4	37.4	51.3
	60	19.8	4.7	9.1	66.4	54.7
E. coli K12 *fepA*	0	100.0	0.0	0.0	0.0	100
	7.5	99.7	0.1	0.1	0.0	97.5
	15	99.1	0.3	0.7	0.0	94.7
	30	85.1	12.5	2.0	0.4	93.2
	60	51.2	37.6	10.4	0.7	87.3

Table S3. Antibacterial activity of cisplatin, L-EP and D-EP based on OD_{600} (mean ± standard deviation).

Strain	[cisplatin] (μM)	OD_{600}	[L-EP] (μM)	OD_{600}	[D-EP] (μM)	OD_{600}
E. coli CFT073	0	0.25±0.008	0	0.21±0.02	0	0.20±0.02
	7.5	0.23±0.02	7.5	0.16±0.02	0.01	0.20±0.01
	15	0.19±0.01	15	0.16±0.02	0.1	0.15±0.02
	30	0.12±0.02	30	0.14±0.03	1	0.086±0.02
	60	0.10±0.02	60	0.13±0.01	10	0.052±0.01
E. coli CFT073 *fepC*	0	0.29±0.03	0	0.28±0.008	0	0.31±0.05
	7.5	0.29±0.02	7.5	0.32±0.03	0.01	0.30±0.02
	15	0.27±0.05	15	0.32±0.02	0.1	0.33±0.02
	30	0.15±0.05	30	0.29±0.02	1	0.30±0.04
	60	0.026±0.02	60	0.25±0.03	10	0.29±0.05
E. coli CFT073 *fepDG*	0	0.32±0.03	0	0.28±0.007	0	0.30±0.03
	7.5	0.30±0.02	7.5	0.33±0.05	0.01	0.31±0.03
	15	0.22±0.04	15	0.30±0.03	0.1	0.32±0.02
	30	0.058±0.04	30	0.28±0.03	1	0.29±0.07
	60	0.015±0.008	60	0.23±0.03	10	0.28±0.05
E. coli CFT073 *fes*	0	0.30±0.02	0	0.30±0.05	0	0.30±0.03
	7.5	0.29±0.01	7.5	0.20±0.04	0.01	0.30±0.05
	15	0.32±0.07	15	0.13±0.05	0.1	0.28±0.01
	30	0.23±0.06	30	0.088±0.04	1	0.25±0.05
	60	0.040±0.02	60	0.069±0.02	10	0.085±0.04
E. coli CFT073 *iroD*	0	0.30±0.004	0	0.28±0.05	0	0.28±0.03
	7.5	0.30±0.01	7.5	0.26±0.04	0.01	0.28±0.02
	15	0.30±0.02	15	0.20±0.01	0.1	0.25±0.01
	30	0.35±0.06	30	0.15±0.01	1	0.14±0.04
	60	0.022±0.007	60	0.09±0.01	10	0.043±0.02
E. coli K12	0	0.25±0.04	0	0.19±0.02	0	0.22±0.03
	7.5	0.25±0.07	7.5	0.16±0.03	0.01	0.21±0.02
	15	0.21±0.06	15	0.15±0.01	0.1	0.065±0.01
	30	0.15±0.004	30	0.13±0.007	1	0.040±0.005
	60	0.075±0.02	60	0.14±0.006	10	0.034±0.01
E. coli K12 *fepA*	0	0.18±0.03	0	0.13±0.02	0	0.15±0.01
	7.5	0.15±0.04	7.5	0.28±0.1	0.01	0.15±0.02
	15	0.13±0.04	15	0.21±0.1	0.1	0.14±0.03
	30	0.10±0.03	30	0.17±0.1	1	0.11±0.007
	60	0.060±0.02	60	0.16±0.1	10	0.12±0.02

Supporting Figures

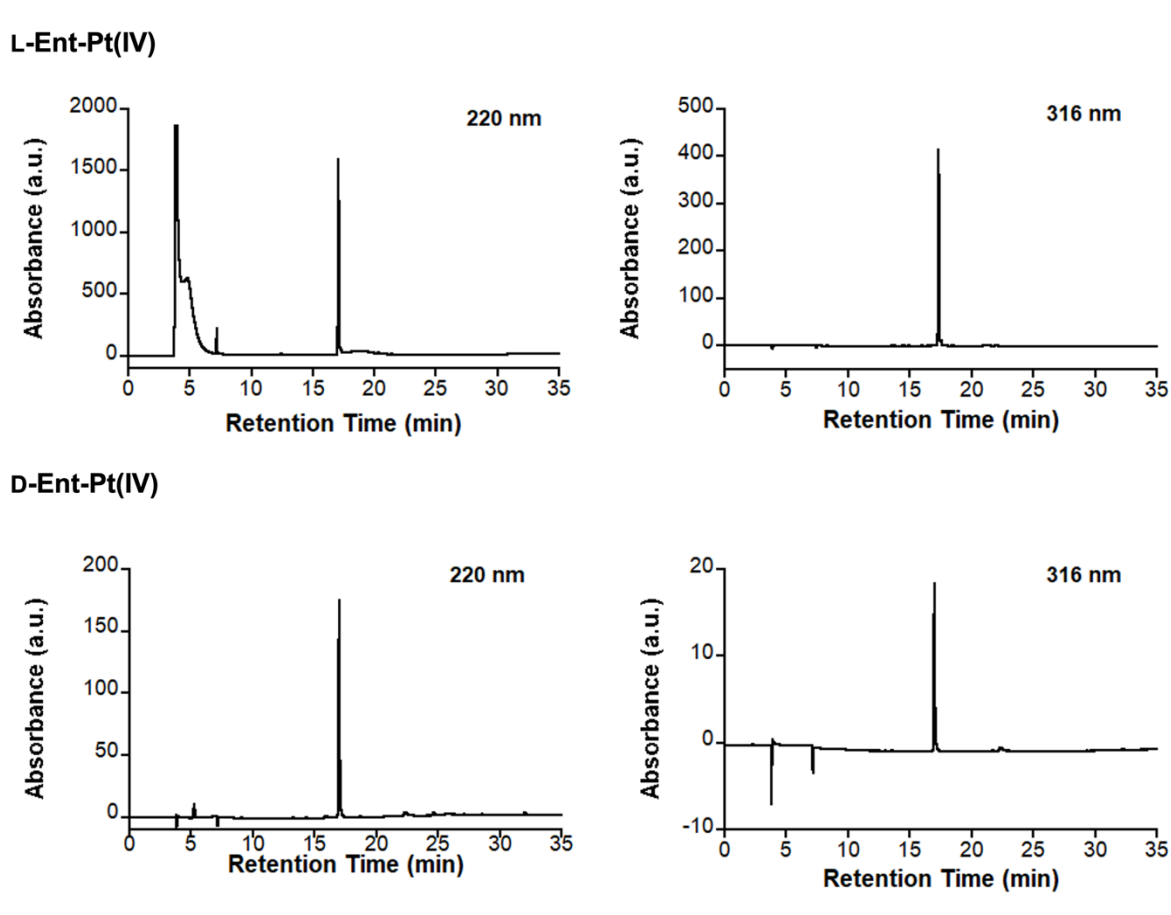

Figure S1. Analytical HPLC traces of purified L- and D-EP. The peak at ca. 5 min in the 220 nm trace of L-EP is DMSO.

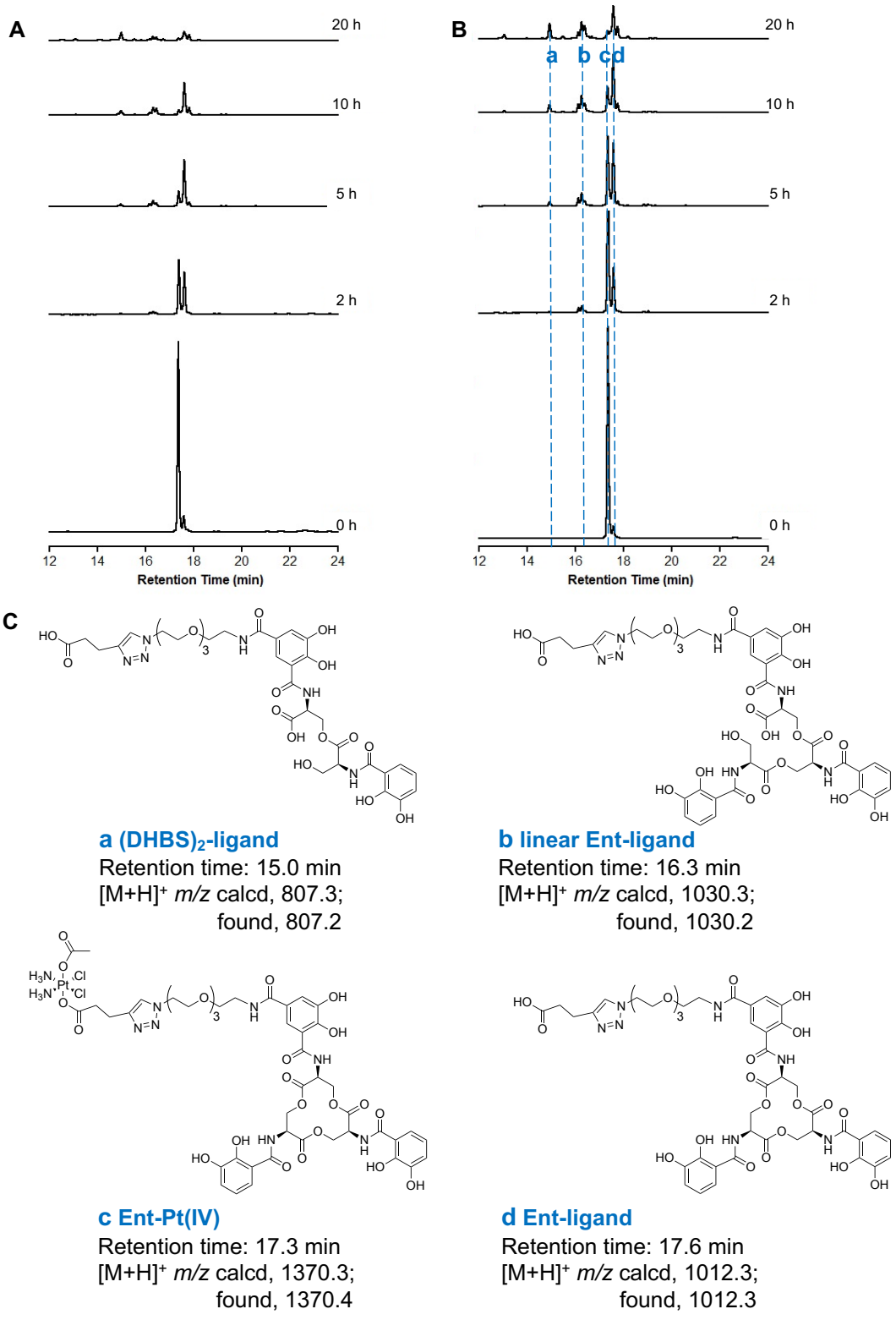

Figures S2. Analytical HPLC traces (220 nm absorption) of L-EP decomposition in the modified M9 medium with **(A)** 16.5 μg/mL thiamine and **(B)** 0.6 μg/mL thiamine at 30 °C. **(C)** Compounds detected by LC/MS. DHBS, 2,3-dihydroxybenzoyl serine

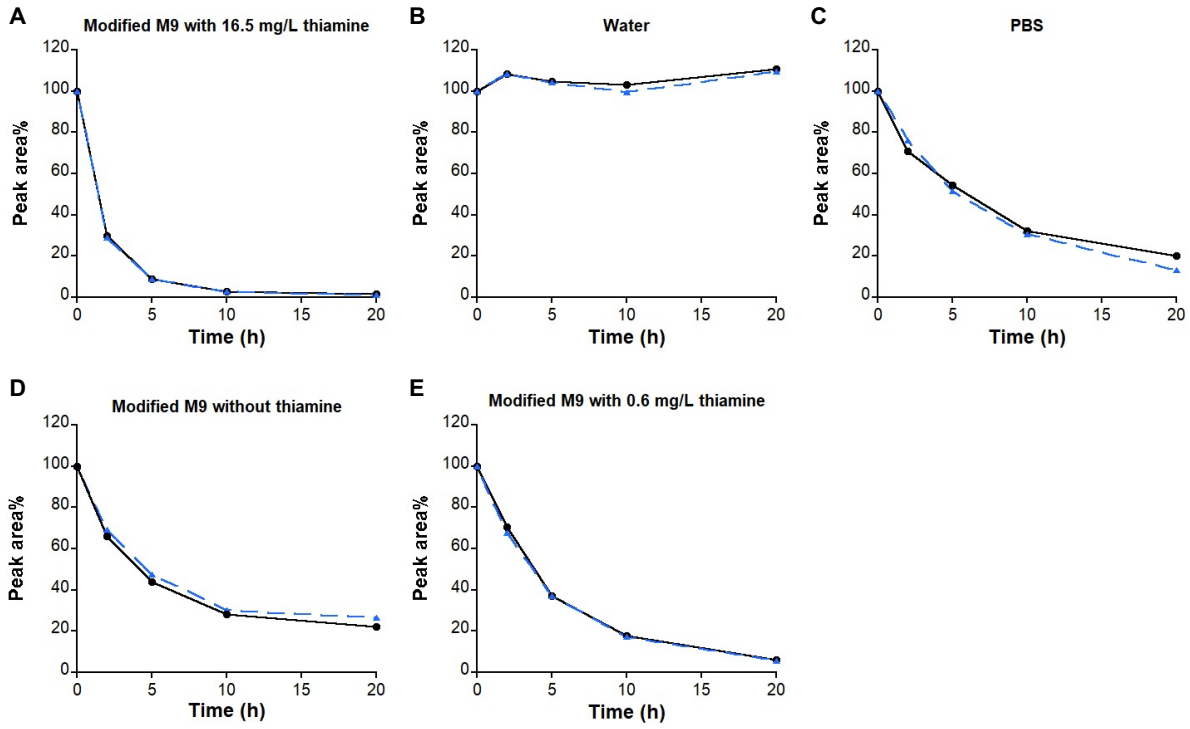

Figures S3. Stability of L-EP in **(A)** modified M9 medium with 16.5 μg/mL thiamine, **(B)** water, **(C)** PBS, modified M9 medium **(D)** without thiamine and **(E)** with 0.6 μg/mL thiamine at 30 °C. Stability was determined by integrating the peak area of L-EP in each sample and normalizing it to that of the sample at t = 0 h. Decomposition products were analyzed by LC/MS; black line: 220 nm; blue dash line: 316 nm.

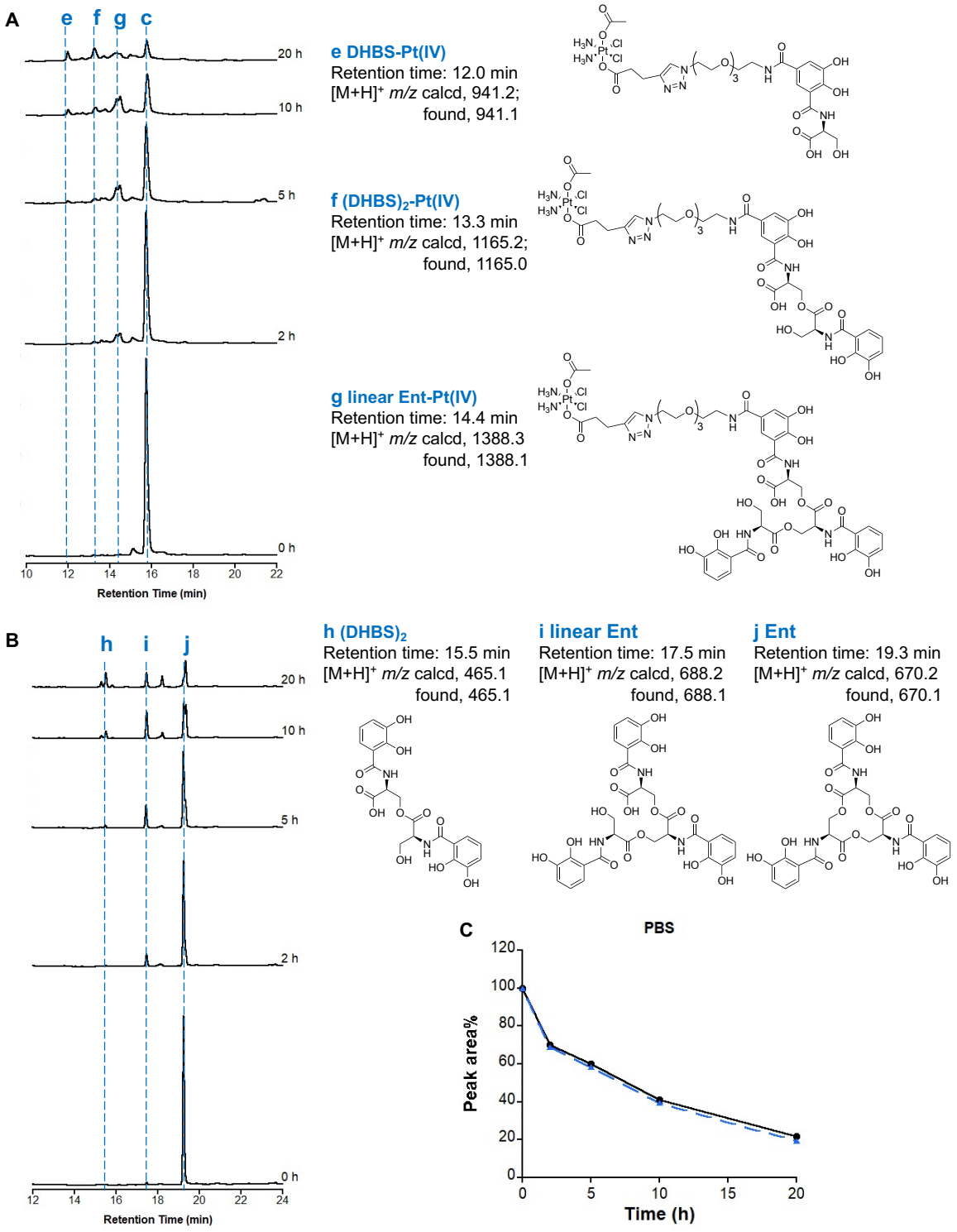

Figure S4. Analytical HPLC traces (220 nm absorption) and LC/MS analysis of **(A)** L-EP and **(B)** Ent decomposition in PBS at 30 °C. **(C)** Stability of Ent in PBS at 30 °C. Stability was determined by integrating the peak area of Ent in each sample and normalizing it to that of the sample at t = 0 h; black line: 220 nm; blue dash line: 316 nm. DHBS, 2,3-dihydroxybenzoyl serine. Note: the retention time of L-EP **c** was shifted to 15.8 min.

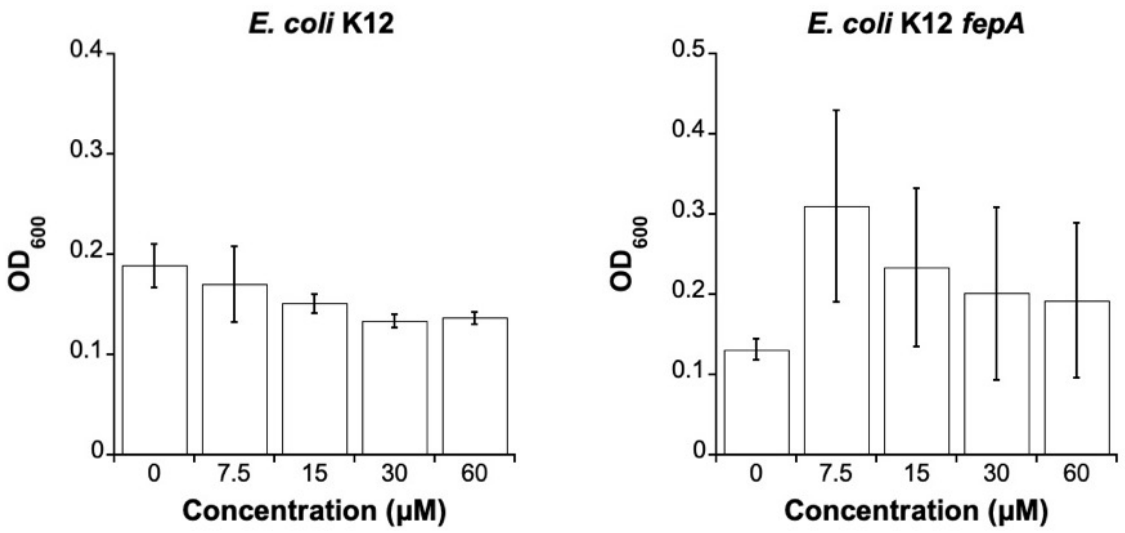

Figure S5. Antibacterial activity of L-EP against *E. coli* K12 and its *fepA* mutant based on OD_{600} (data shown in **Table S3**). All assays were performed in modified M9 medium (11 h, 30 °C, 500 rpm; mean ± standard deviation; n ≥ 4). The same data for K12 were also presented as relative OD_{600} (%) in **Figure 3A**.

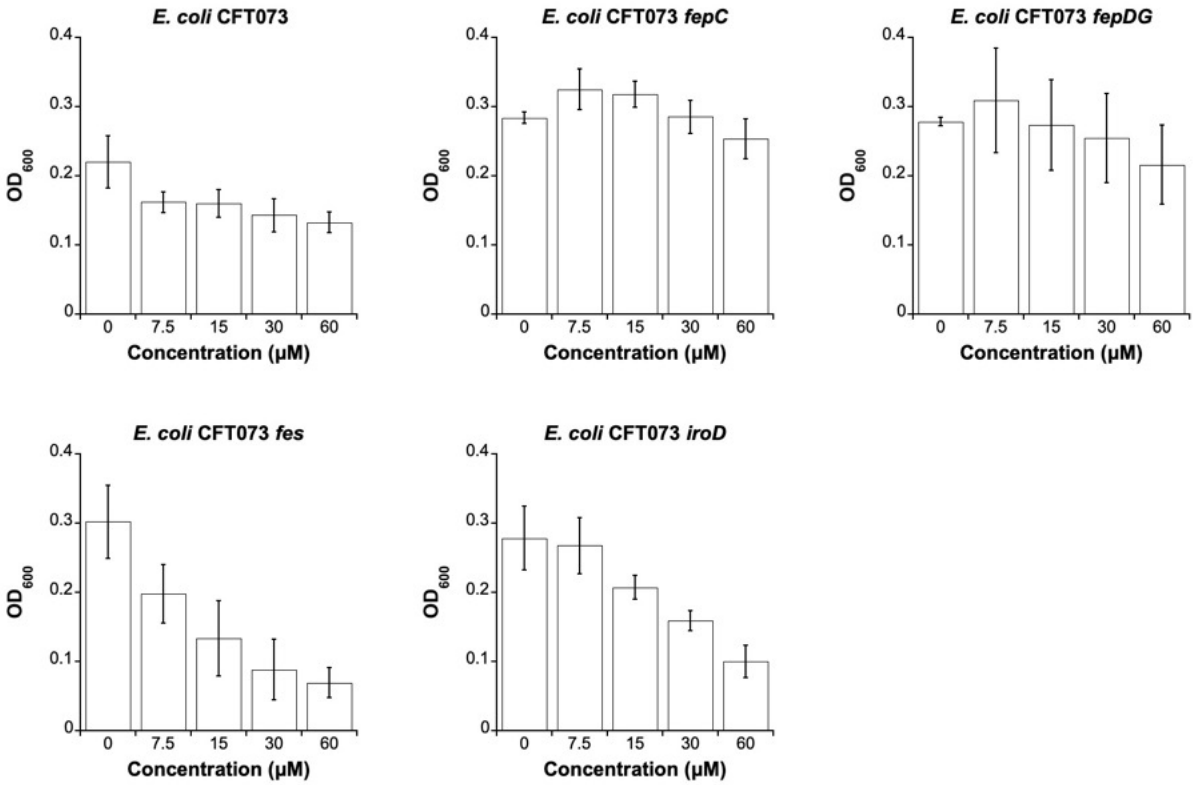

Figure S6. Antibacterial activity of L-EP against *E. coli* CFT073 and its *fepC, fepDG, fes,* and *iroD* mutants based on OD_{600} (data shown in **Table S3**). All assays were performed in modified M9 medium (11 h, 30 °C, 500 rpm; mean ± standard deviation, n ≥ 6). The same data for CFT073 were also presented as relative OD_{600} (%) in **Figures 3A, 6A and 7A**. The same data for the *fes* mutant were also presented as relative OD_{600} (%) in **Figure 6B**.

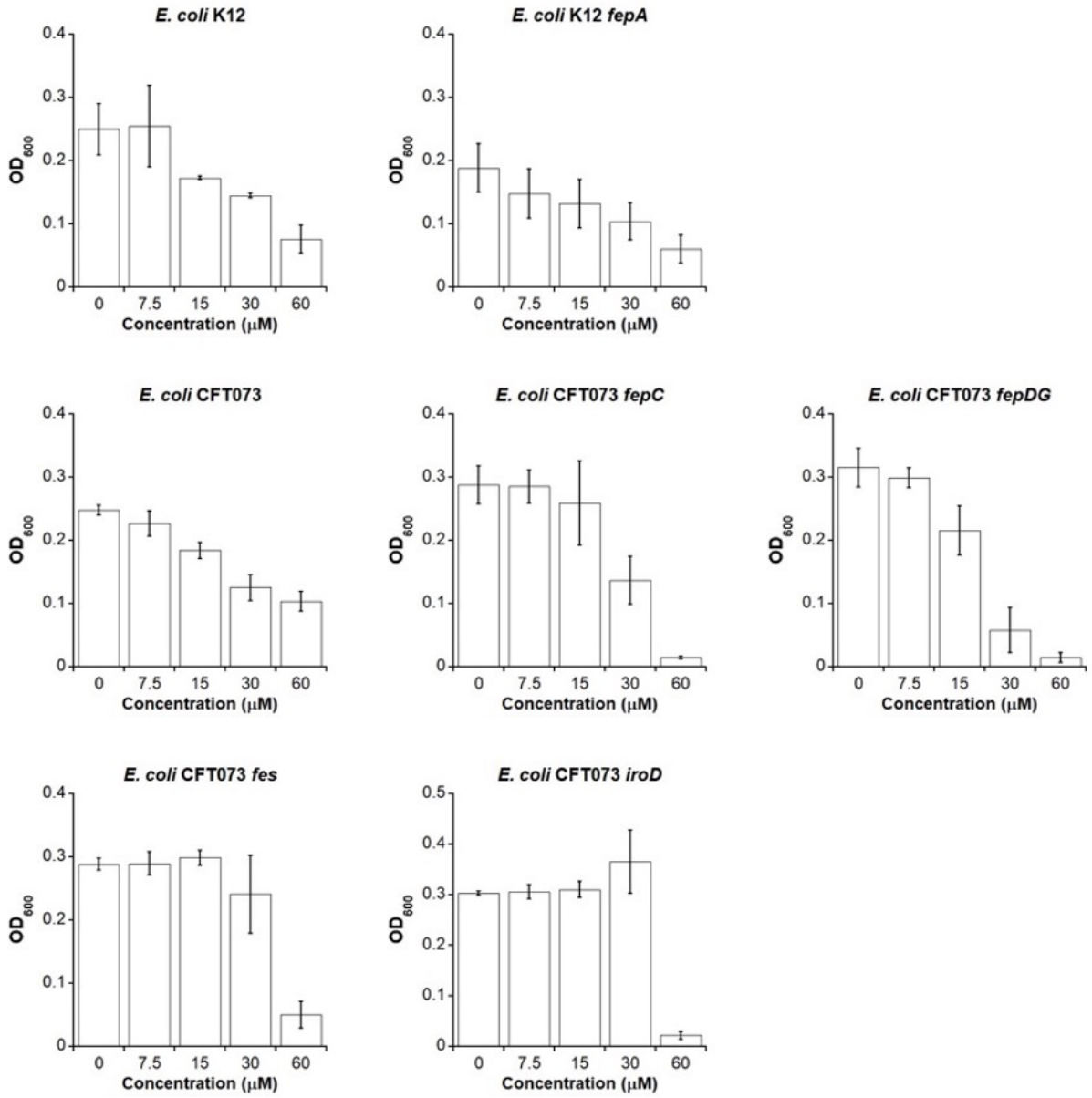

Figure S7. Antibacterial activity of cisplatin against *E. coli* K12 and its *fepA* mutant; *E. coli* CFT073 and its *fepC, fepDG, fes* and *iroD* mutants based on OD_{600} (data shown in **Table S3**). All assays were performed in modified M9 medium (11 h, 30 °C, 500 rpm; mean ± standard deviation, n ≥ 4). The same data for K12 were also presented as relative OD_{600} (%) in **Figure 3A**. The same data for CFT073 were also presented as relative OD_{600} (%) in **Figures 3A and 7A**.

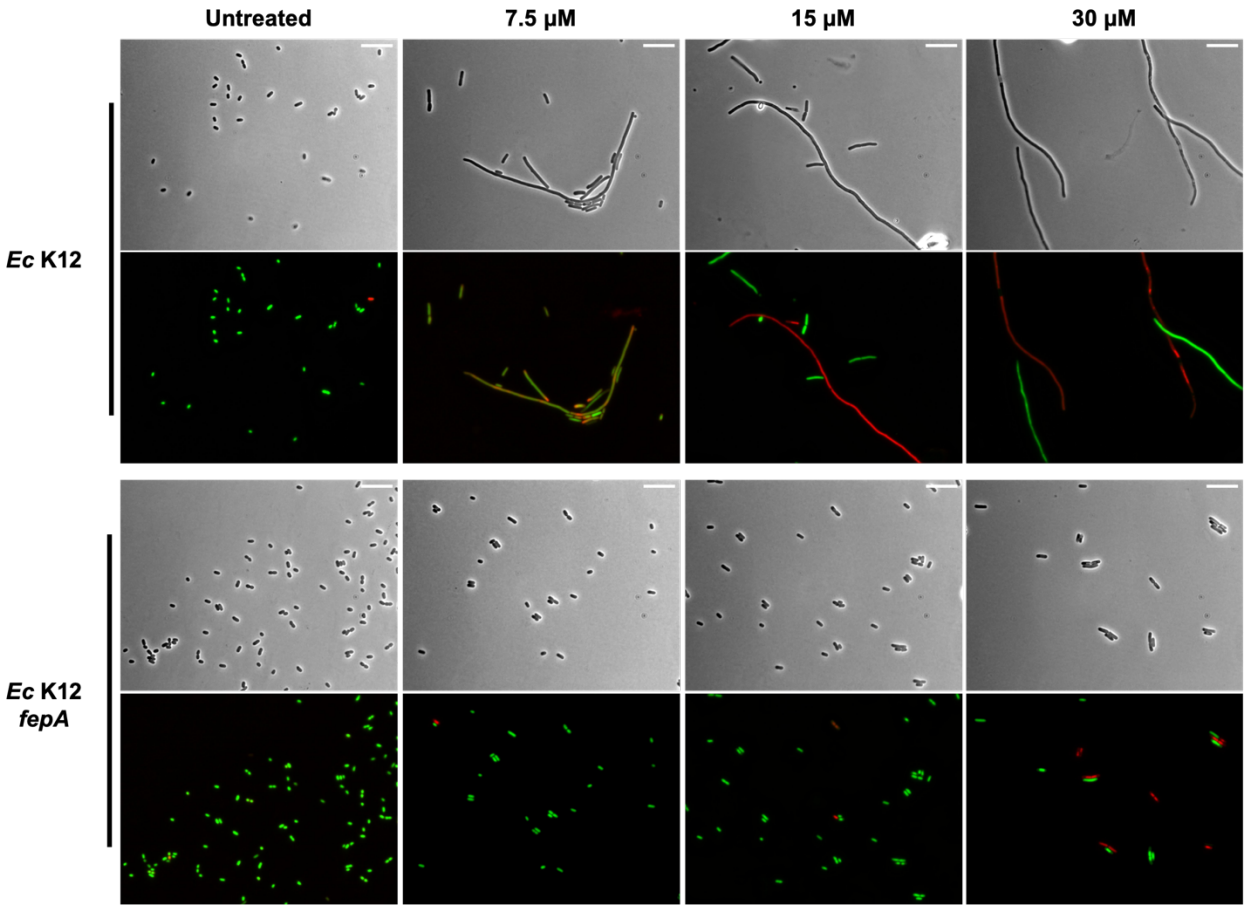

Figure S8. Representative phase-contrast and fluorescence micrographs of *E. coli* K12 and its *fepA* mutant treated with L-EP (scale bar = 10 µm).

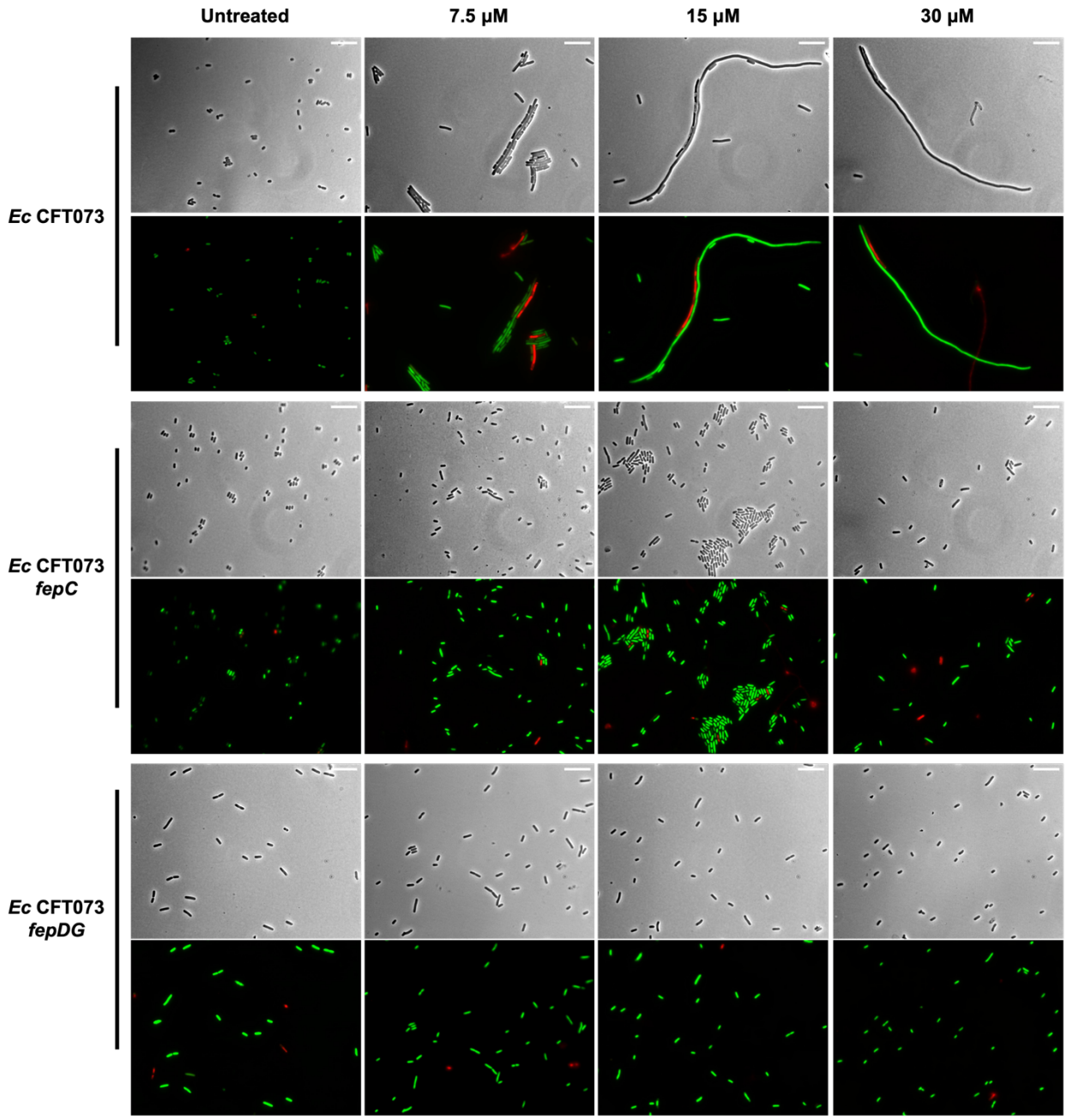

Figure S9. Representative phase-contrast and fluorescence micrographs of *E. coli* CFT073 and its *fepC* and *fepDG* mutants treated with L-EP (scale bar = 10 μm).

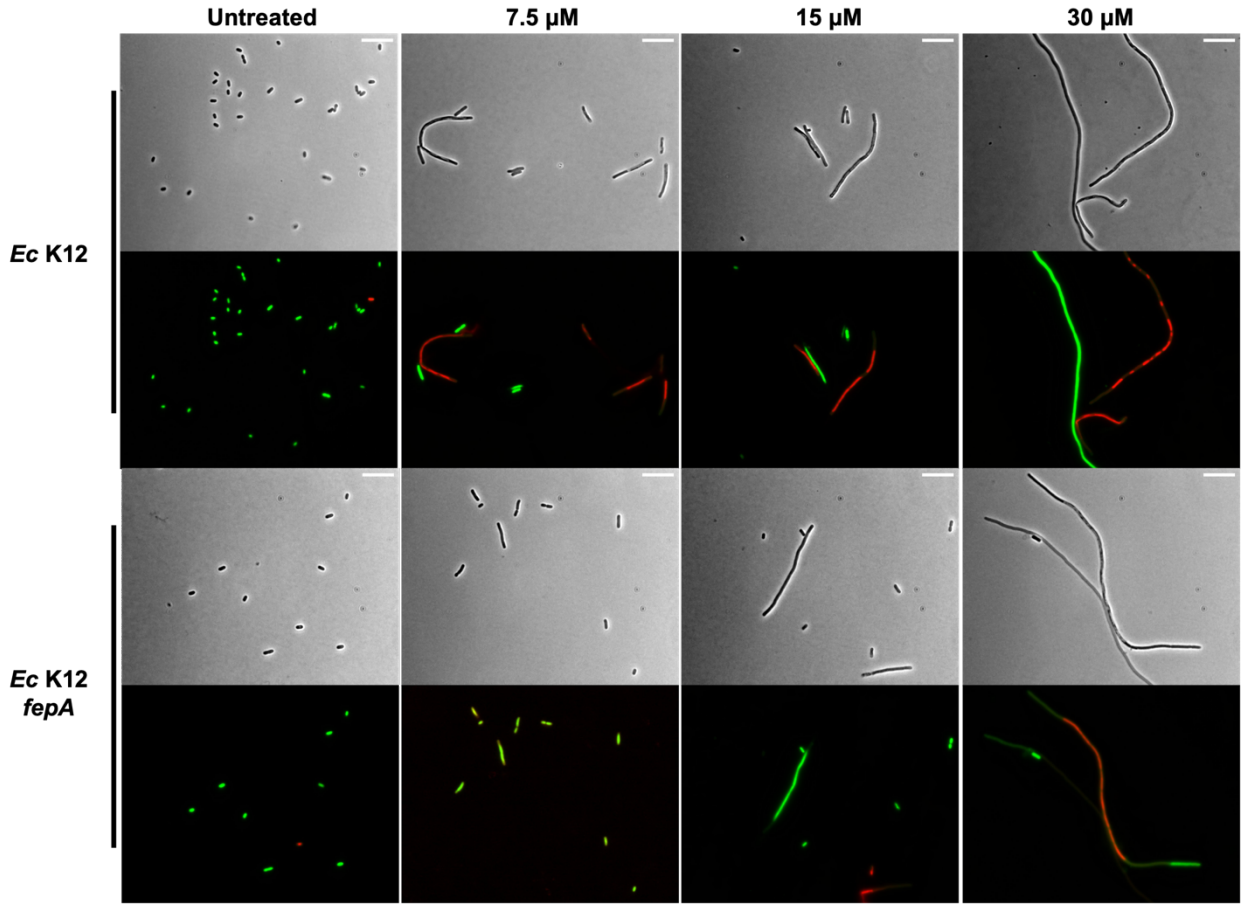

Figure S10. Representative phase-contrast and fluorescence micrographs of *E. coli* K12 and its *fepA* mutant treated with cisplatin (scale bar = 10 μm).

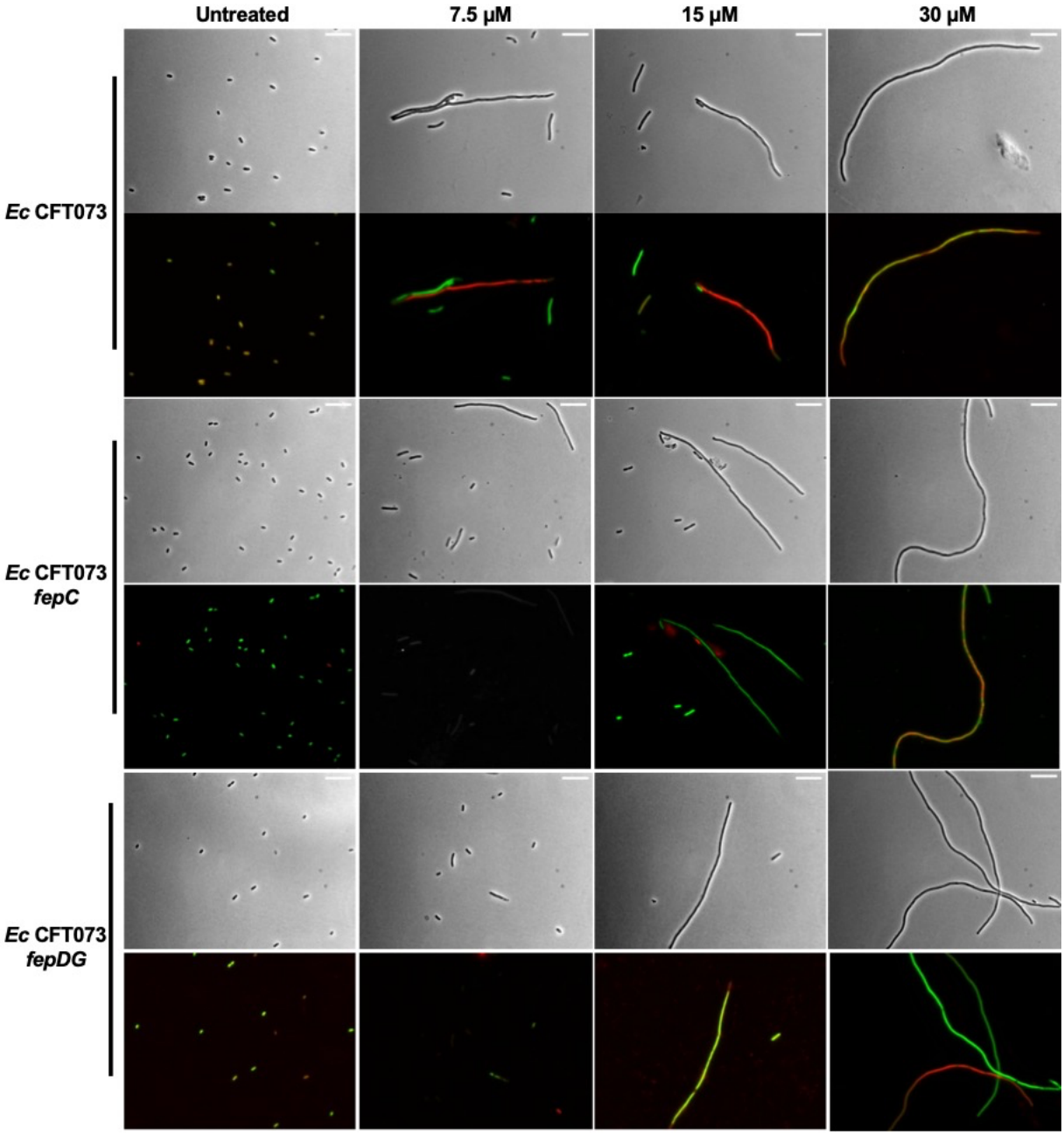

Figure S11. Representative phase-contrast and fluorescence micrographs of *E. coli* CFT073 and its *fepC* and *fepDG* mutants treated with cisplatin (scale bar = 10 μm).

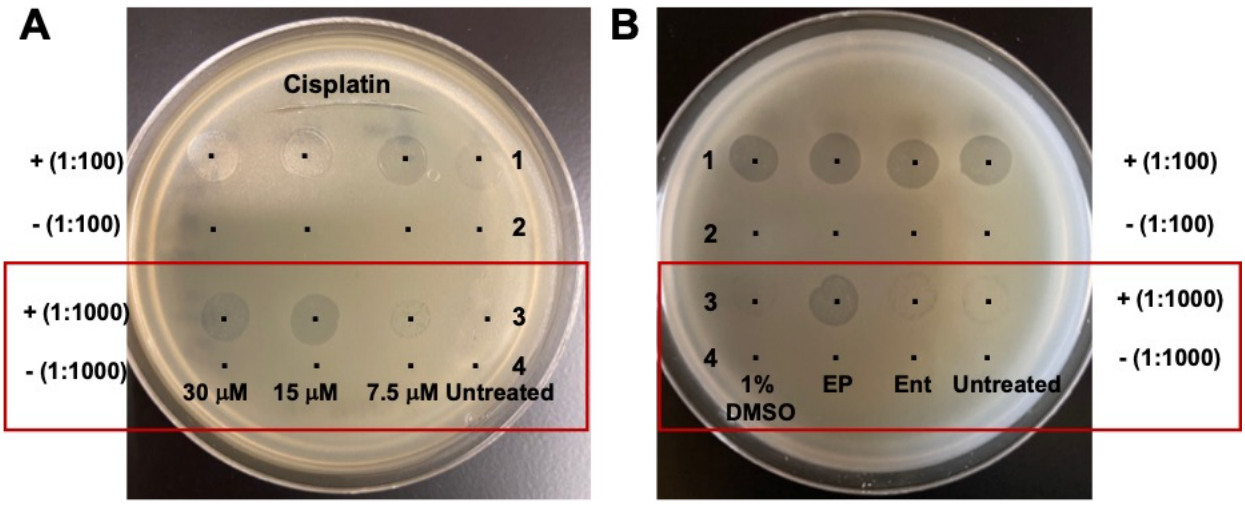

Figure S12. Effect of L-EP on lysogenic *E. coli*. Representative images of the development of plaques in a lawn of non-lysogenic *E. coli* CFT073 following application of 10 μL drops of 100-fold (row **1** and **2**) and 1000-fold (row **3** and **4**, in the red frame) diluted suspensions of treated *E. coli* W3104 (+) and solutions containing only the corresponding compound (-). **(A)** *E. coli* W3104 treated with cisplatin (0–30 μM). **(B)** *E. coli* W3104 treated with 15 μM L-EP, 15 μM Ent, 1% DMSO and the untreated control. We note that plaque formation was observed in all 100-fold diluted suspensions, including the untreated sample, which was presumably due to a small portion of lysogenic bacteria that enter the lytic cycle under normal growth condition.

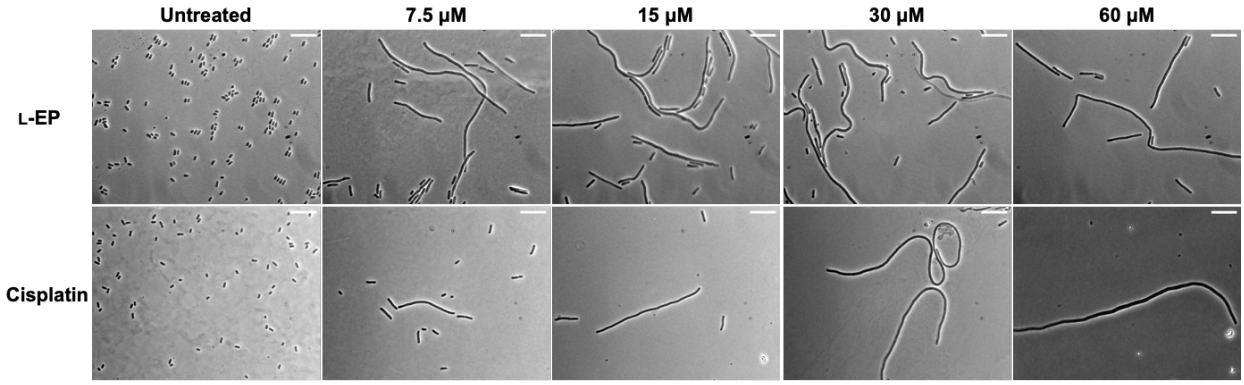

Figure S13. Representative phase-contrast micrographs of *E. coli* CFT073 *fepA iroN* mutant treated with L-EP (top) and cisplatin (bottom) (scale bar = 10 μm).

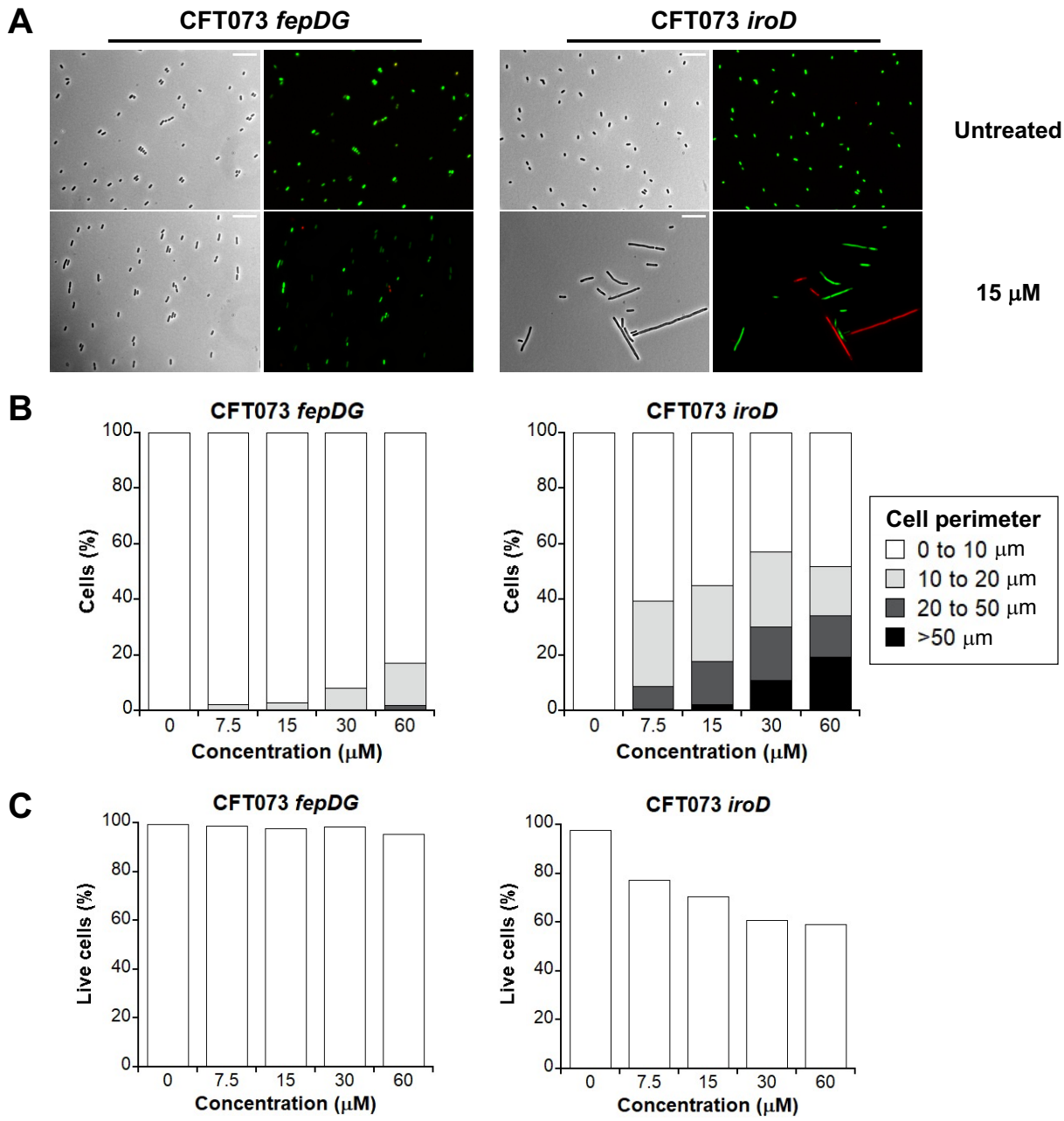

Figure S14. Activity of L-EP against *E. coli* CFT073 *fepDG* and *iroD* mutants. **(A)** Representative phase-contrast and fluorescence micrographs of *E. coli* CFT073 *fepDG* and *iroD* mutants treated with 15 μM L-EP in modified M9 medium for 11 h at 30 °C. Scale bar: 10 μm. **(B)** Quantification of the L-EP-induced bacterial morphologies in *E. coli*. **(C)** Viability of *E. coli* determined by LIVE/DEAD staining. For morphology and viability quantification, 500–1000 cells were manually counted for each condition from micrographs. For morphology quantification, cell size was measured and grouped by perimeter.

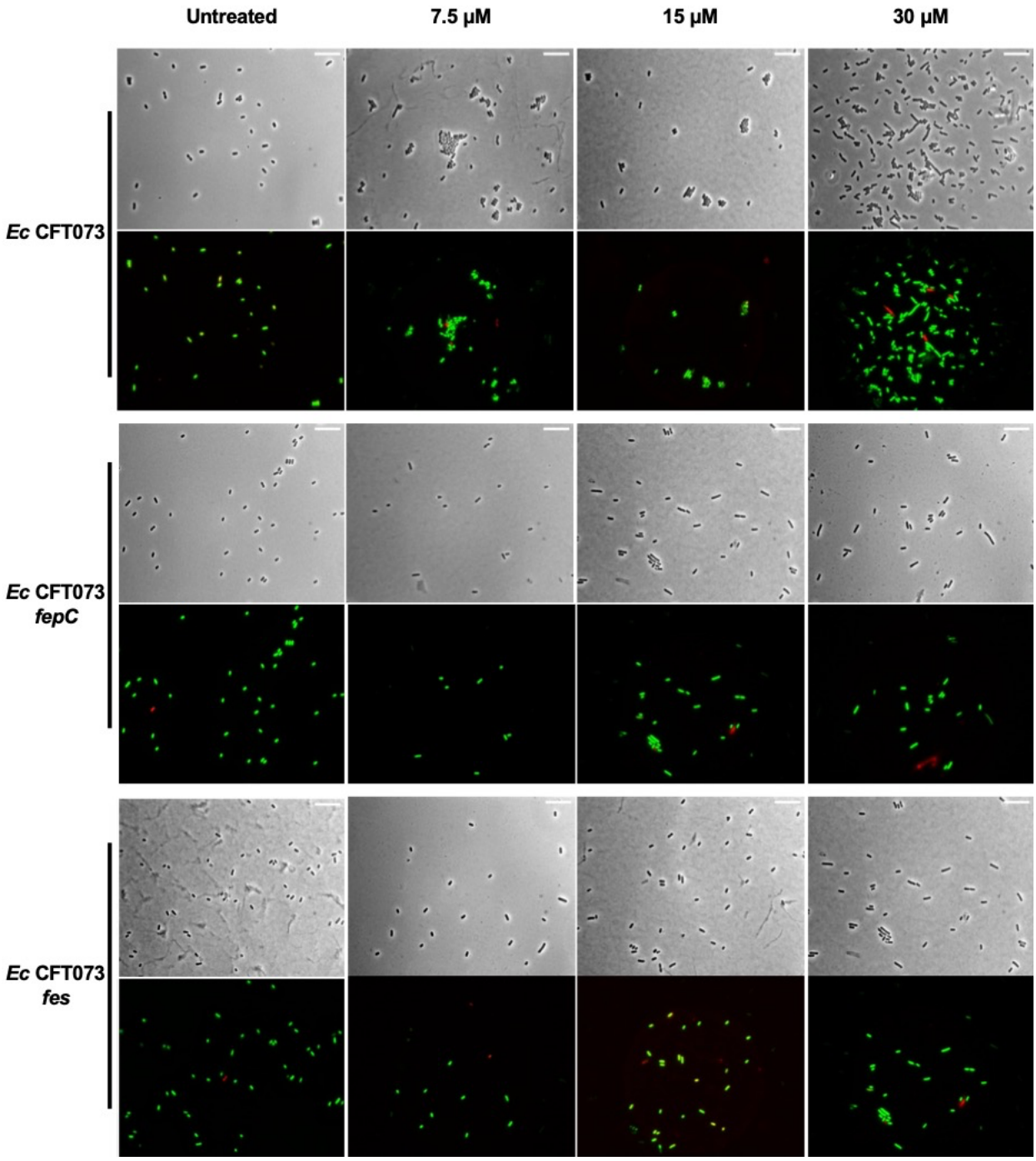

Figure S15. Representative phase-contrast and fluorescence micrographs of *E. coli* CFT073 and its *fepC* and *fes* mutants treated with Pt(IV)-alkyne (scale bar = 10 μm).

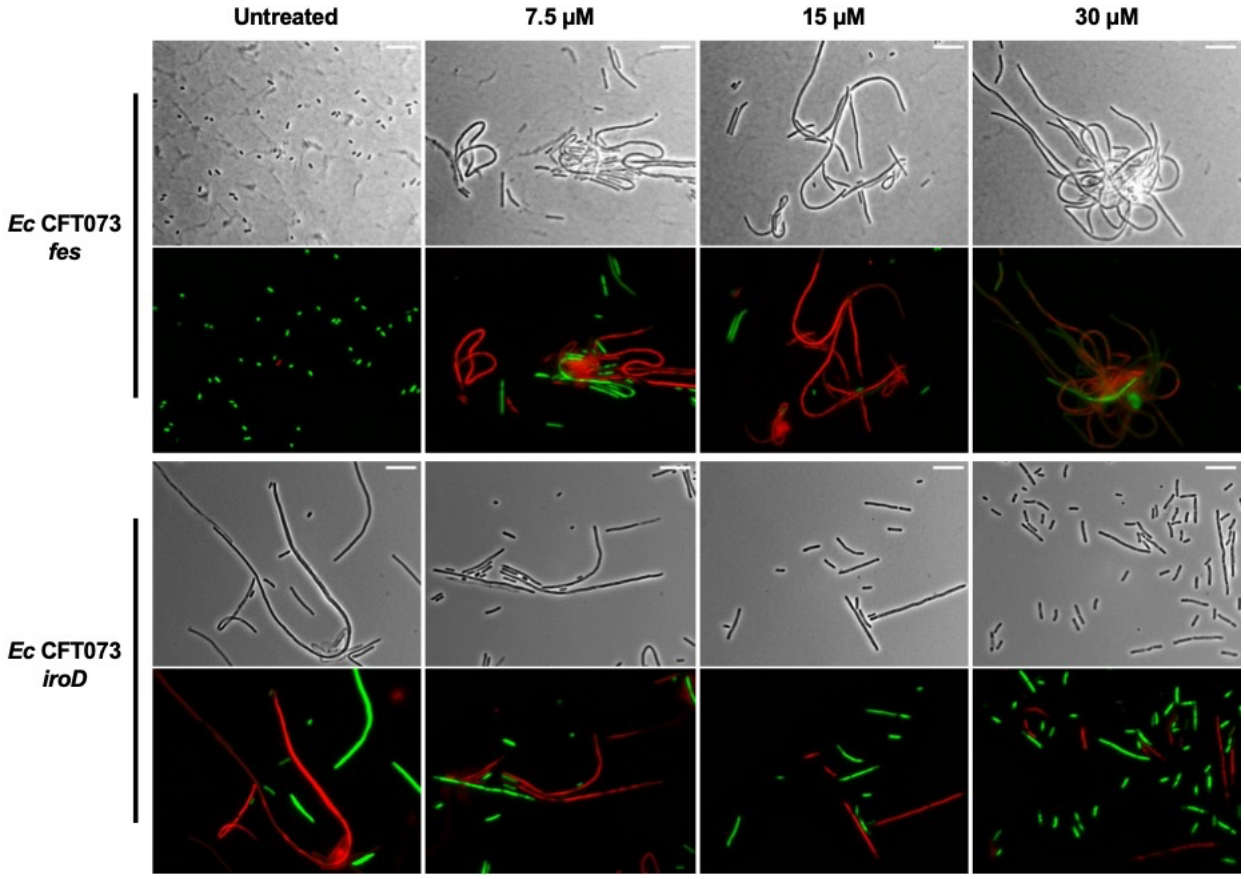

Figure S16. Representative phase-contrast and fluorescence micrographs of *E. coli* CFT073 and its *fes* and *iroD* mutants treated with L-EP (scale bar = 10 μm).

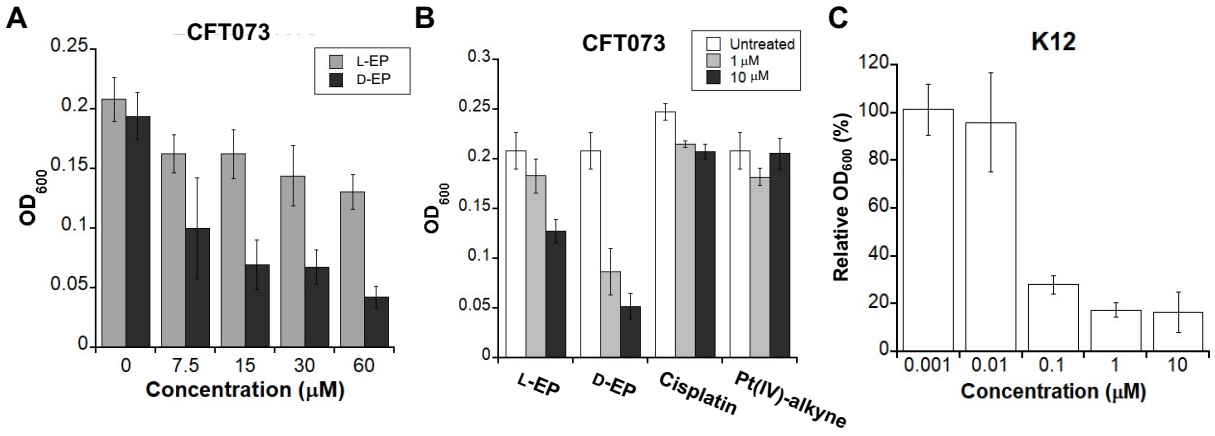

Figure S17. Antibacterial activity of D-EP against *E. coli* CFT073 and K12. **(A)** Antibacterial activity of L-EP (n=7) and D-EP (n=6) against *E. coli* CFT073 based on OD_{600}. **(B)** Comparison of the antibacterial activity of L-EP, D-EP, cisplatin and Pt(IV)-alkyne at 1 μM and 10 μM, respectively (mean ± standard deviation, n=3; the untreated control in L-EP, D-EP and Pt(IV)-alkyne refers to treating bacteria with 1% DMSO in modified M9 medium; the untreated control in cisplatin refers to incubating bacteria in modified M9 medium). **(C)** Antibacterial activity of D-EP against *E. coli* K12 (mean ± standard deviation, n = 4); relative OD_{600} refers to the OD_{600} value of the treated sample divided by that of the untreated control. All assays were performed in modified M9 medium at 30 °C for 11 h.

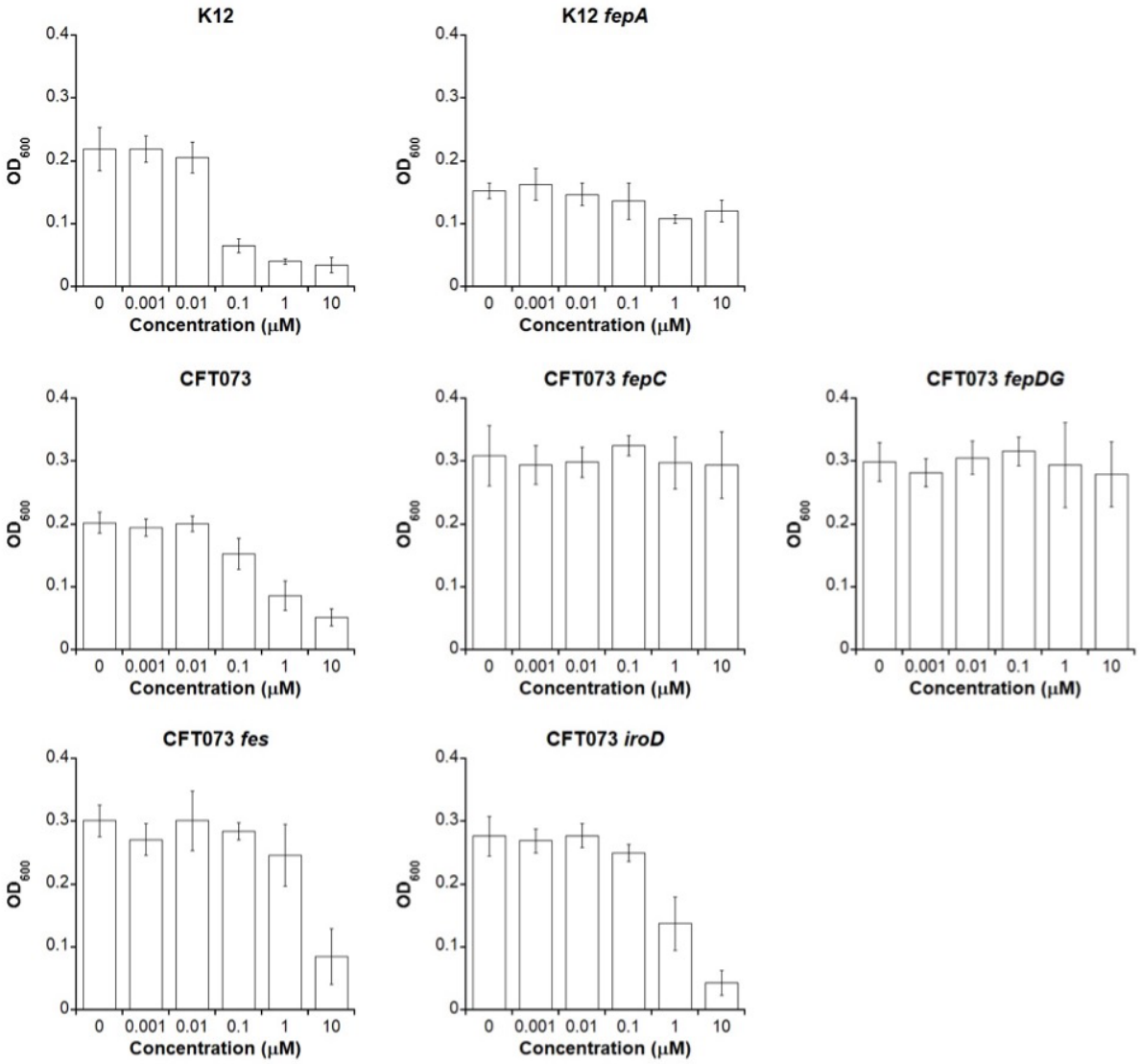

Figure S18. Antibacterial activity of D-EP against *E. coli* K12 and its *fepA* mutant; *E. coli* CFT073 and its *fepC, fepDG, fes* and *iroD* mutants based on OD_{600} (data shown in **Table S3**). All assays were performed in modified M9 medium (11 h, 30 °C, 500 rpm; mean ± standard deviation, n ≥ 4). The same data for K12 were also presented as relative OD_{600} (%) in **Figure S17C**. The same data for CFT073 were also presented as relative OD_{600} (%) in **Figure 7B**.

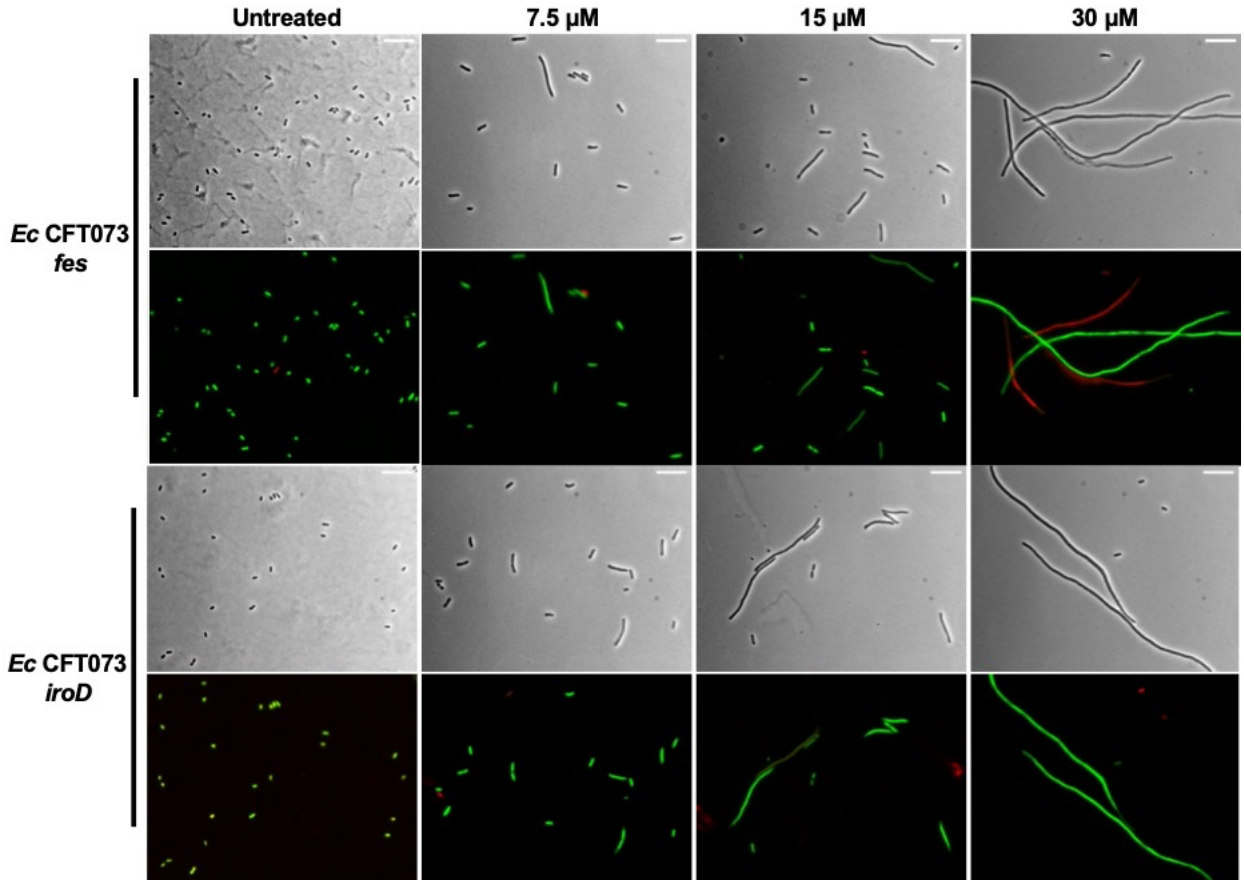

Figure S19. Representative phase-contrast and fluorescence micrographs of *E. coli* CFT073 and its *fes,* and *iroD* mutants treated with cisplatin (scale bar = 10 μm).

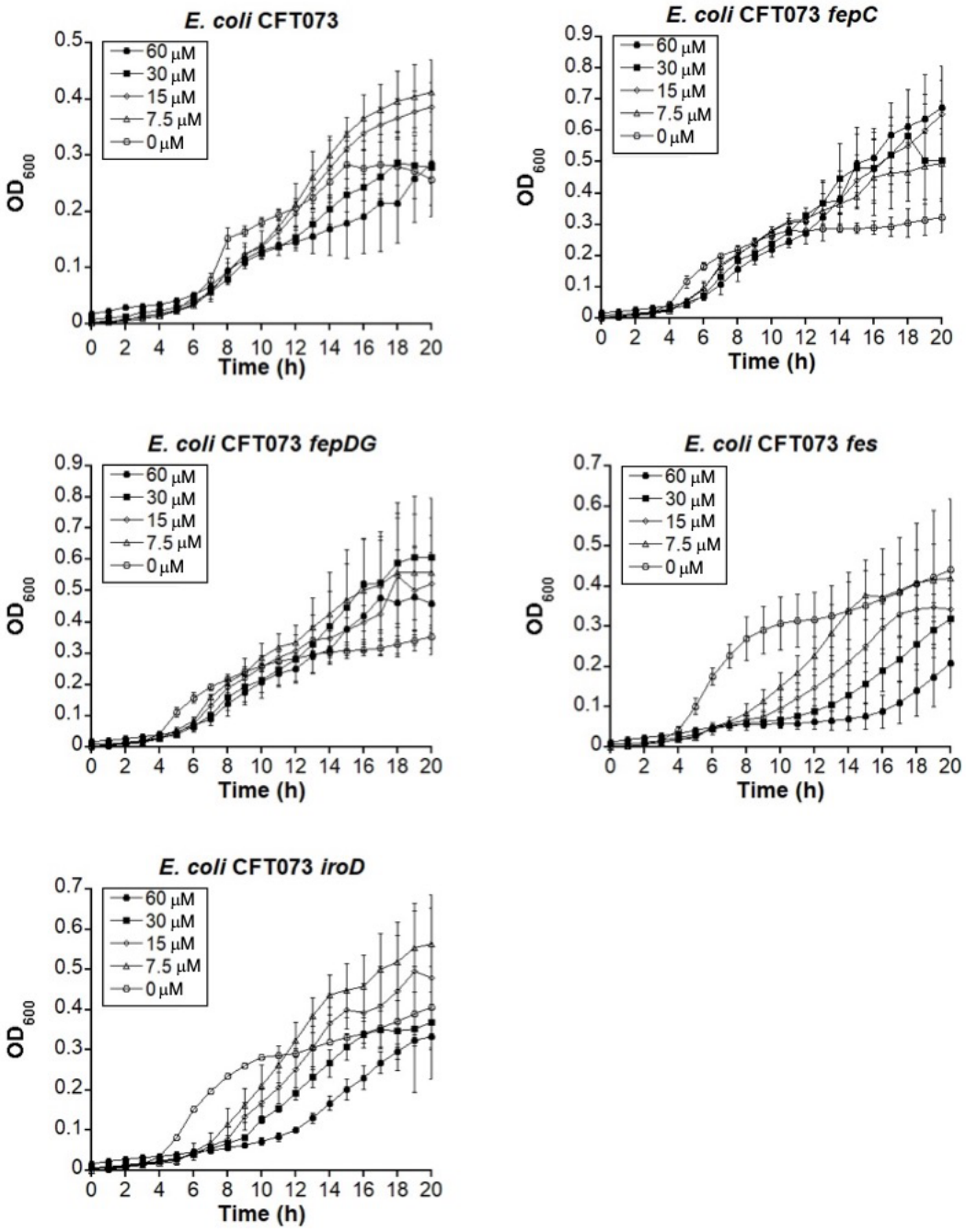

Figure S20. Growth curves of *E. coli* CFT073 and its *fepC, fepDG, fes* and *iroD* mutants treated with L-EP in modified M9 at 30 °C (mean ± standard deviation, n ≥ 3). We note that the large error bars after ~14 h are presumably due to decomposition of L-EP in the modified M9 medium.

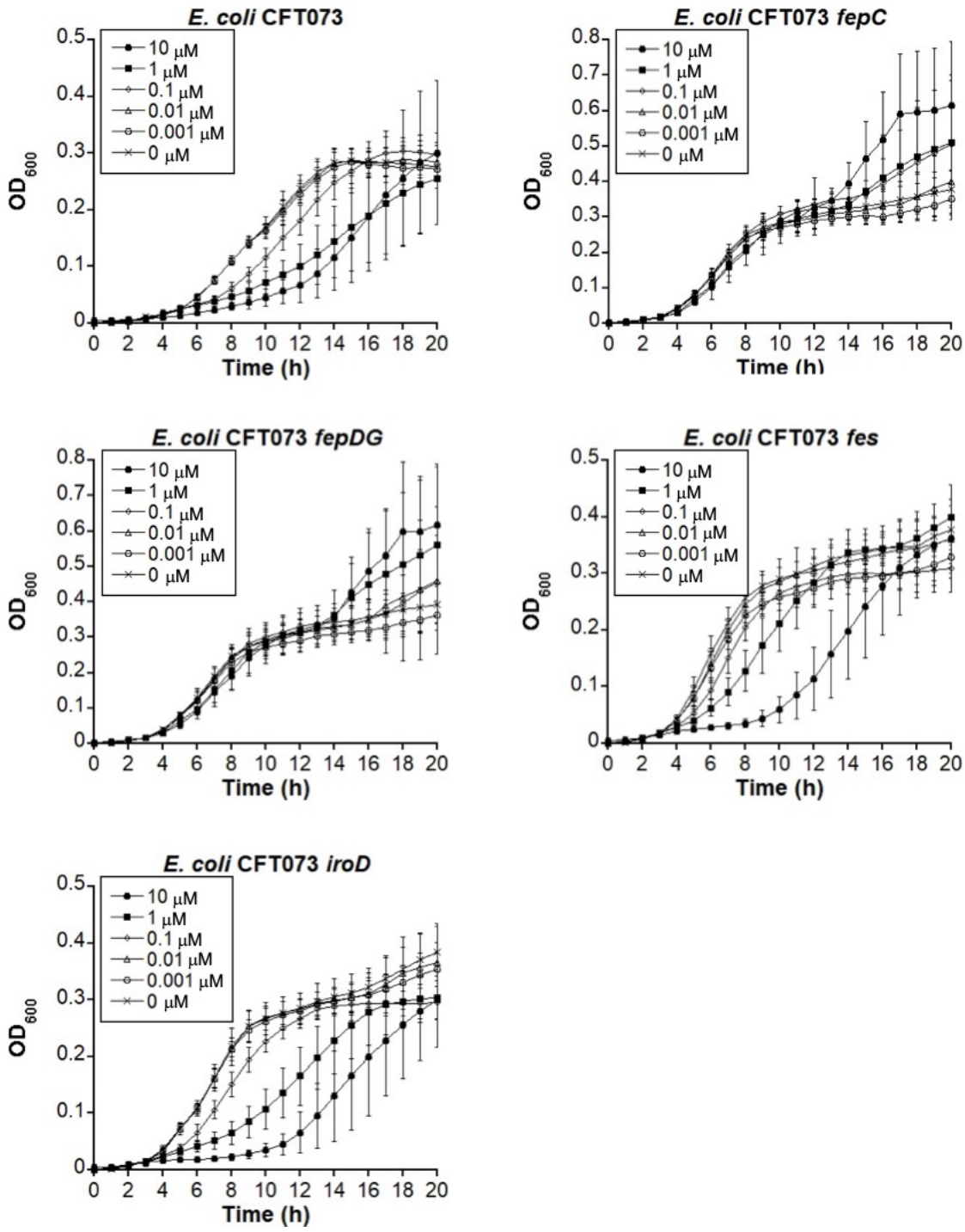

Figure S21. Growth curves of *E. coli* CFT073 and its *fepC, fepDG, fes* and *iroD* mutants treated with D-EP in modified M9 at 30 °C (mean ± standard deviation, n ≥ 3). We note that the large error bars after ~14 h are presumably due to decomposition of D-EP in the modified M9 medium.

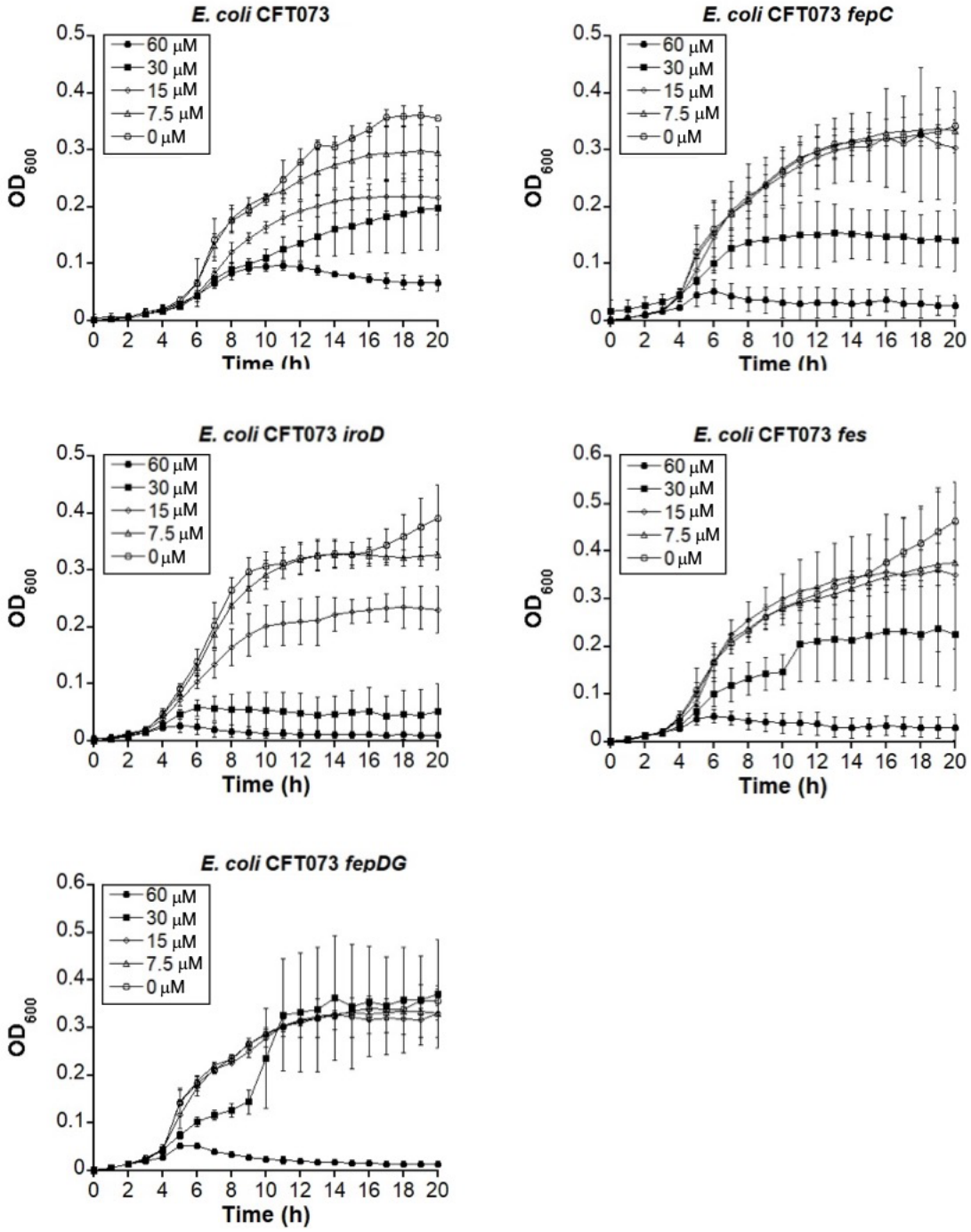

Figure S22. Growth curves of *E. coli* CFT073 and its *fepC, fepDG, fes* and *iroD* mutants treated with cisplatin in modified M9 at 30 °C (mean ± standard deviation, n ≥ 3).

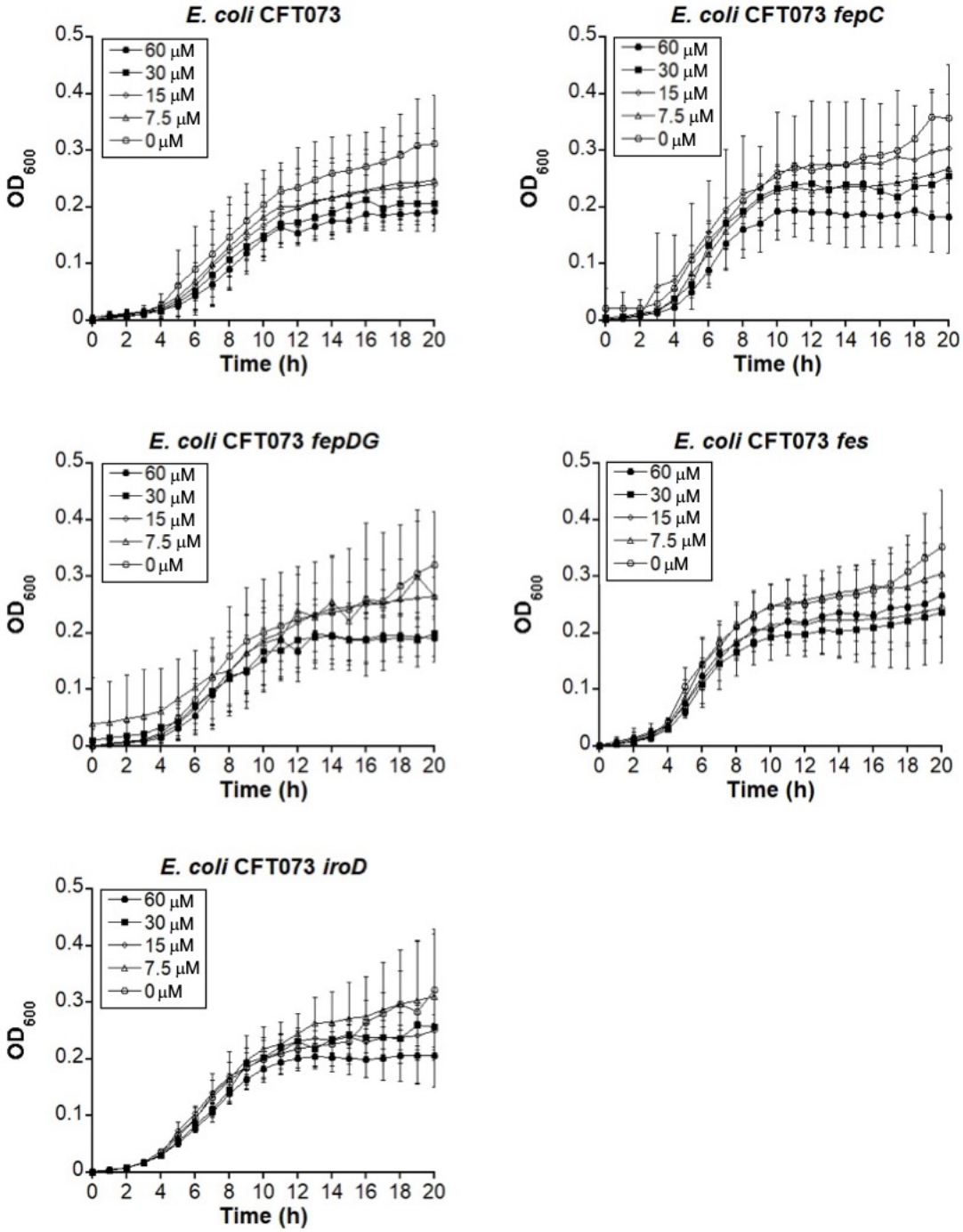

Figure S23. Growth curves of *E. coli* CFT073 and its *fepC, fepDG, fes* and *iroD* mutants treated with Pt(IV)-alkyne in modified M9 at 30 °C (mean ± standard deviation, n ≥ 3)

NMR Spectroscopic Data

NMR spectra of *cis, cis, trans*-[$Pt(NH_3)_2Cl_2(OOCCH_3)(OOCCH_2CH_2C{\equiv}CH)$] (Pt(IV)-alkyne 6) in D_2O

^1H NMR

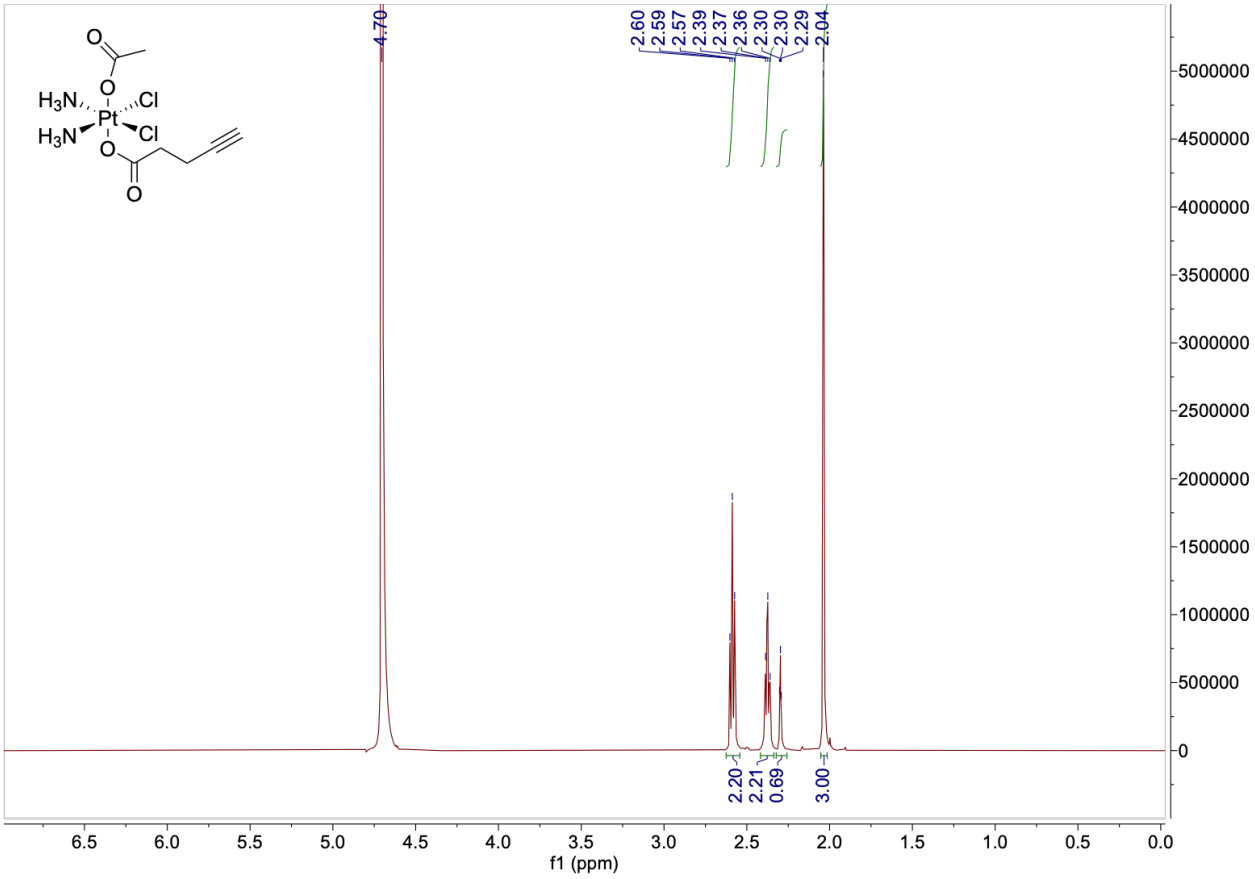

^{195}Pt NMR

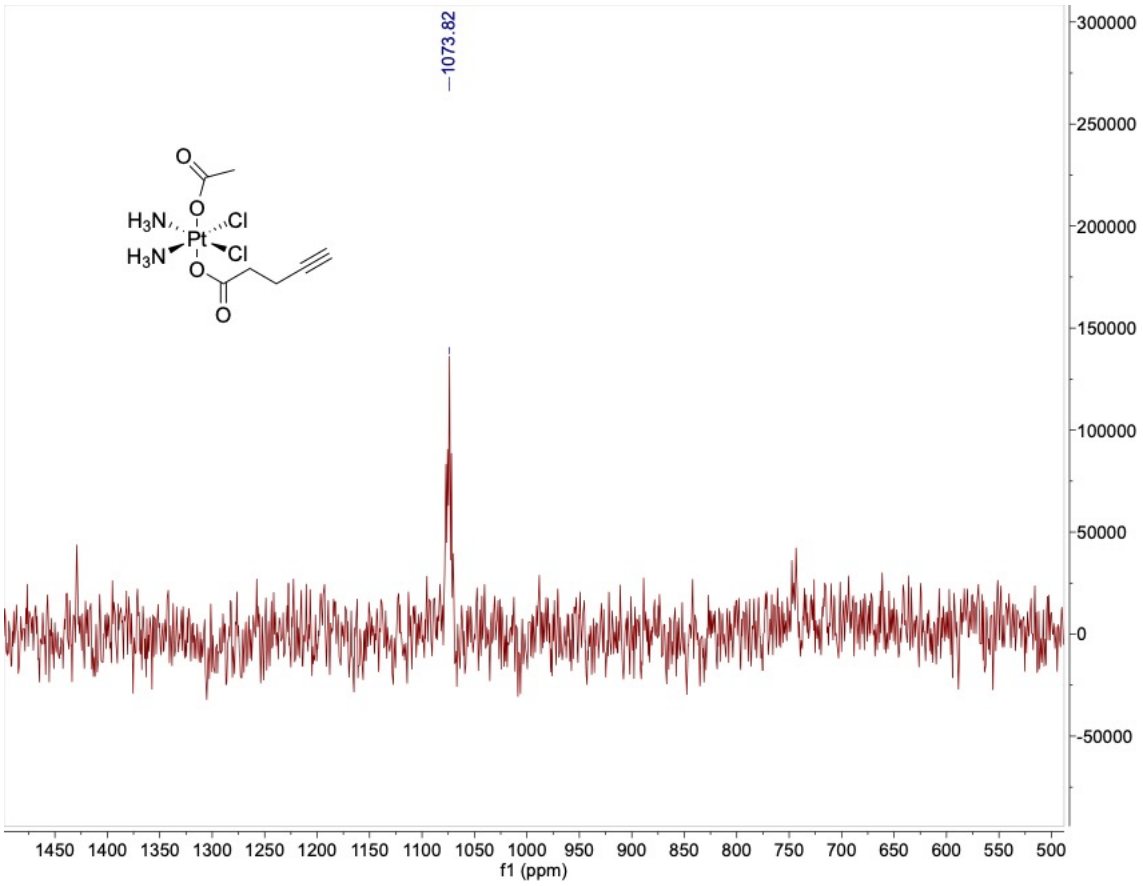
1073.82
300000
250000
200000
150000
100000
50000
0
-50000
1450 1400 1350 1300 1250 1200 1150 1100 1050 1000 950 900 850 800 750 700 650 600 550 500
f1 (ppm)

NMR spectra of L-Ent-Pt(IV) 4 in DMSO-d_6

^{1}H NMR

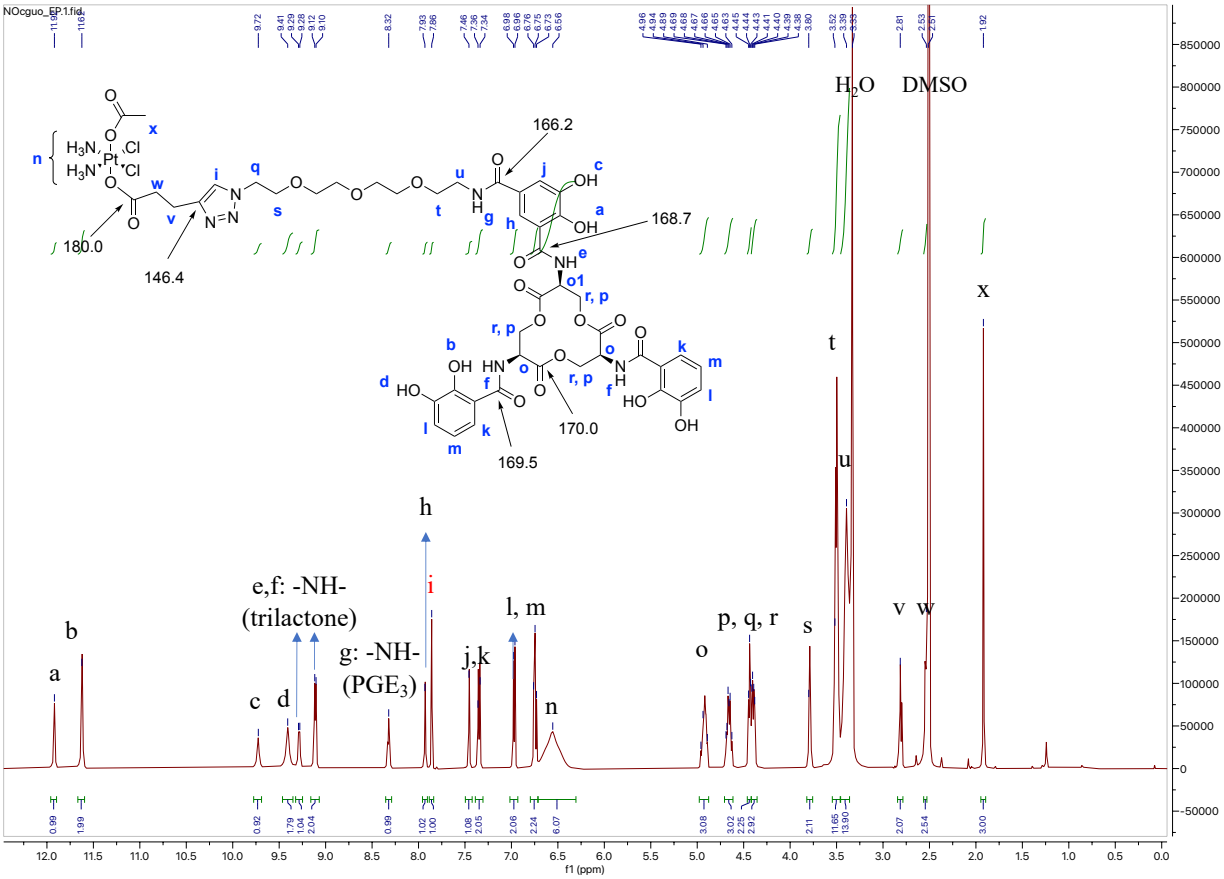

Peak assignment of L-Ent-Pt(IV) **4**

Label	H1	COSY	C13	HMBC	Comments
a	11.92, s			151.1, 146.2, 115.6	
b	11.62, 2H, s			148.9, 146.7, 115.6	
c	9.72, s				
d	9.41, 2H, s				
e	9.29, d	o1		168.8	
f1	9.12, d	o2, o3		169.5, 63.8, 51.5	
f2	9.12, d				
g	8.32, t	u		166.3	
h	7.93, m	j	119.0	168.7, 166.2, 151.1, 118.0	
i	7.86, s		122.9	146.4	
j	7.46, m	h	118.1	166.2, 151.0, 146.1, 118.9	
k1	7.36, d	m; l	118.7	169.5, 149.0, 119.8	
k2	7.36, d				
l1	6.98, d	m; k	119.7	149.0, 146.7, 118.8	
l2	6.98, d				
m1	6.75, t	k, l	118.9	146.7, 115.5; 119.4	
m2	6.75, t				
n	6.56, 6H, br				
o1	4.92, m	e, p, r	51.7	169.9, 63.8	63.8: r,p
o2	4.92, m	f, p, r			
o3	4.92, m				
p1	4.65, m	o, r	63.8	170.0, 51.6	51.5: o
p2	4.65, m				
p3	4.65, m				
q	4.43, 2H, t	s	49.6	122.9, 69.0	122.9: i
r1	4.39, m	o, p	63.8	170.0, 51.6	
r2	4.39, m				
r3	4.39, m				
s	3.80, 2H, t	q	69.2	69.9, 49.6	49.6: q
t	3.52, nH, m	u	69.8, 70.1	70.0, 39.6	overlapping with water peak; integration is off
u	3.39, nH, m	g, t	39.5	166.2, 69.4	
v	2.81, 2H, t	w	22.1	180.2, 146.4, 123.0, 35.7	123.0: i
w	2.53, 2H, t	v	35.8	180.2, 146.4, 21.9	
x	1.92, 3H, s		23.2	178.7	

^{1}H COSY

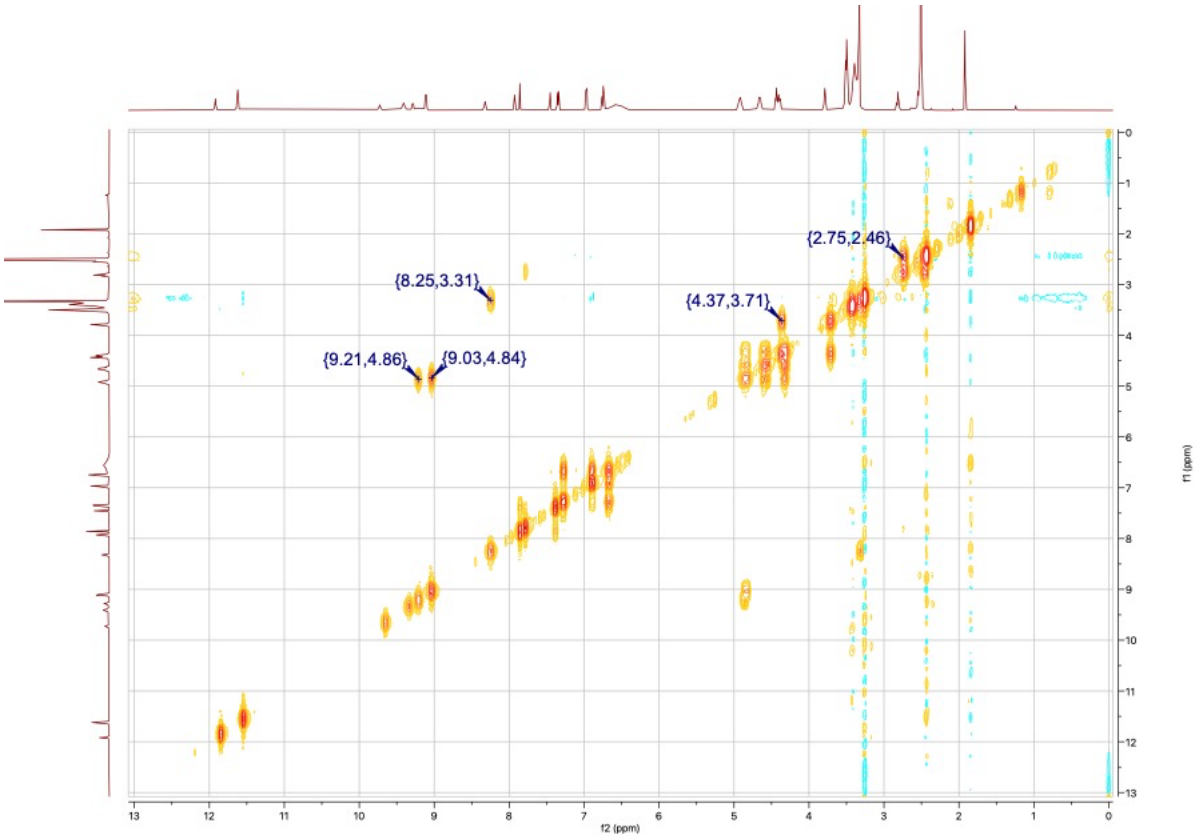

^{1}H-^{13}C HSQC

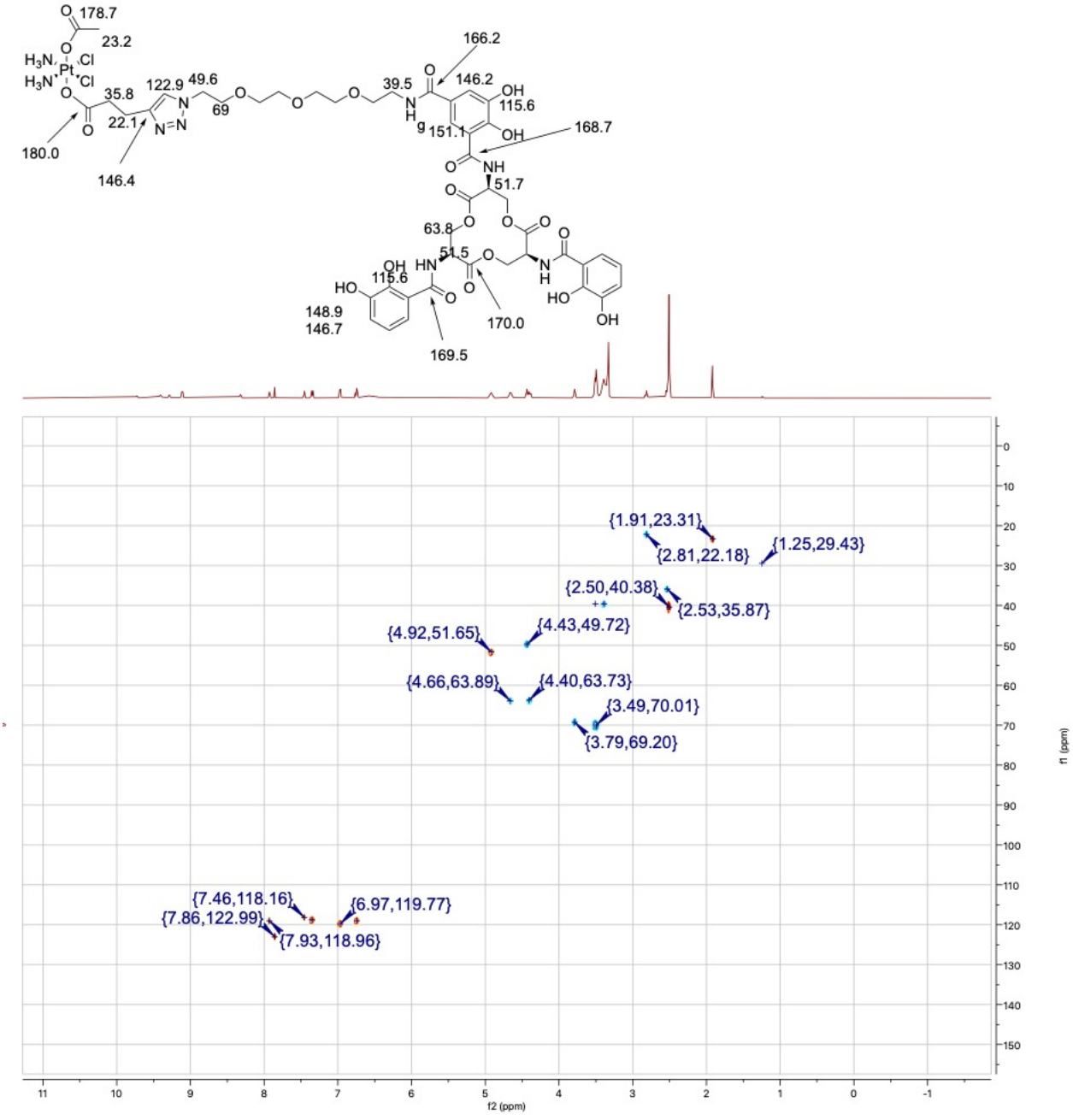
{1.91,23.31}
{2.81,22.18}
{1.25,29.43}
{2.50,40.38}
{2.53,35.87}
{4.92,51.65}
{4.43,49.72}
{4.66,63.89}
{4.40,63.73}
{3.49,70.01}
{3.79,69.20}
{7.46,118.16}
{7.86,122.99}
{6.97,119.77}
{7.93,118.96}
f2 (ppm)
f1 (ppm)

^{1}H-^{13}C HMBC

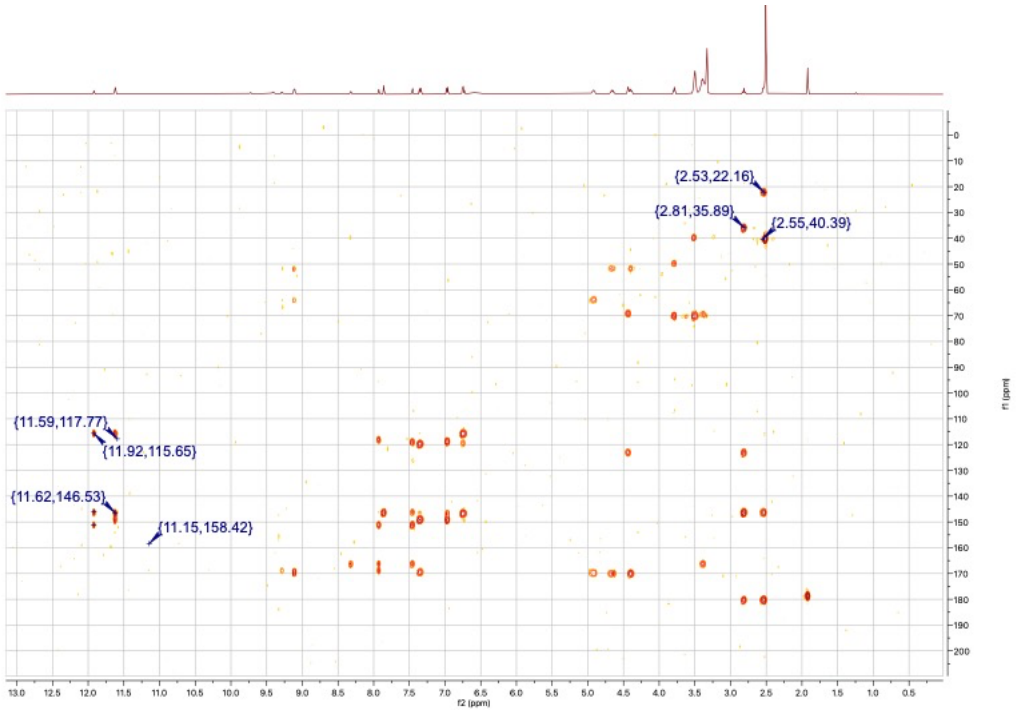

^{1}H-^{195}Pt HMQC

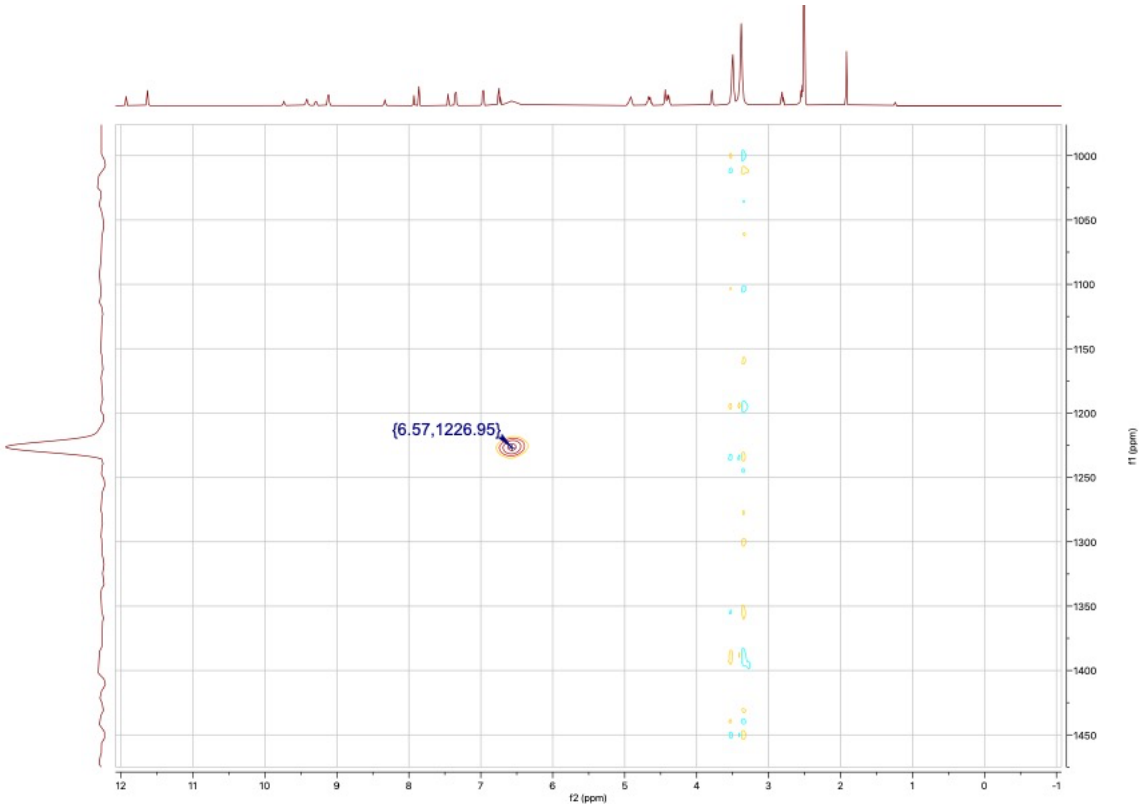

NMR spectra of D-Ent-Pt(IV) in DMSO-d_6

^{1}H NMR

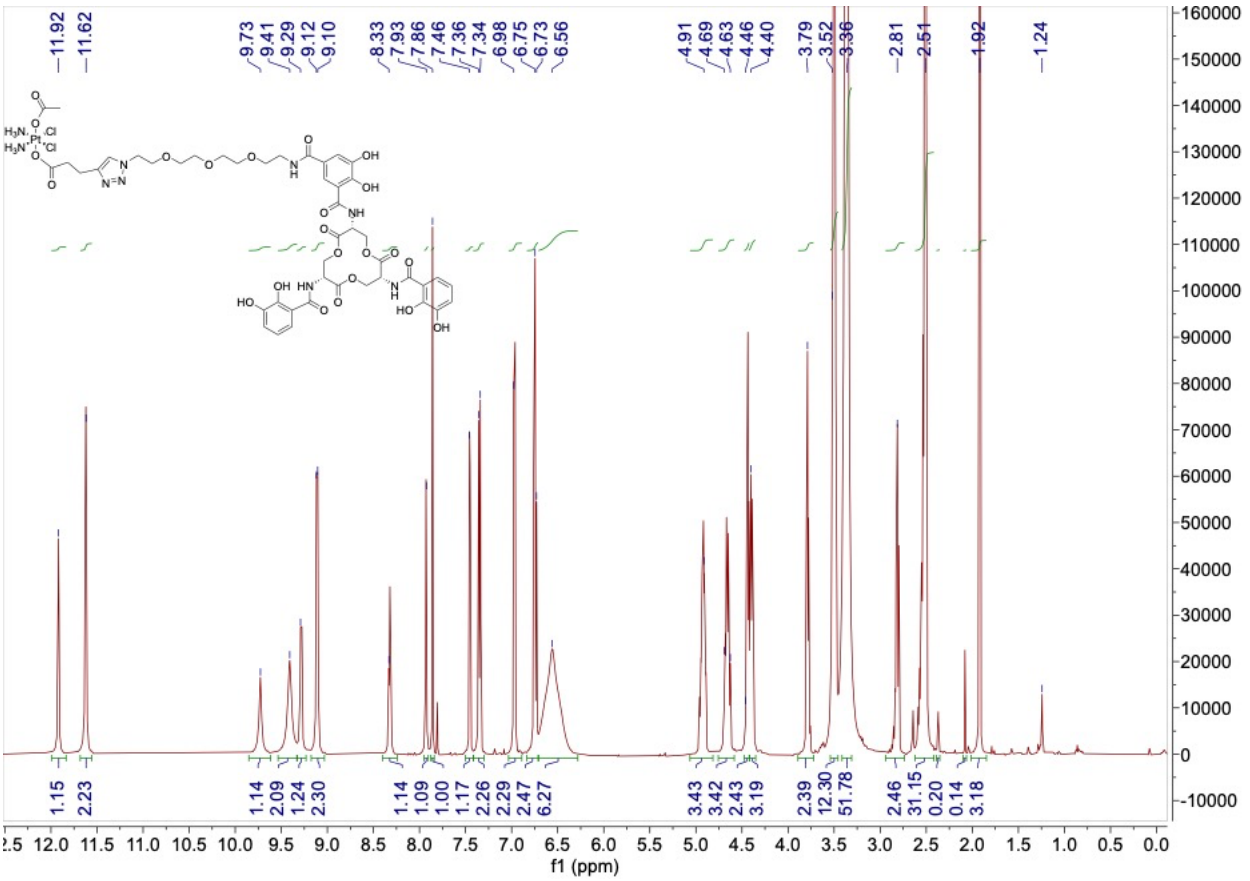

^{1}H COSY

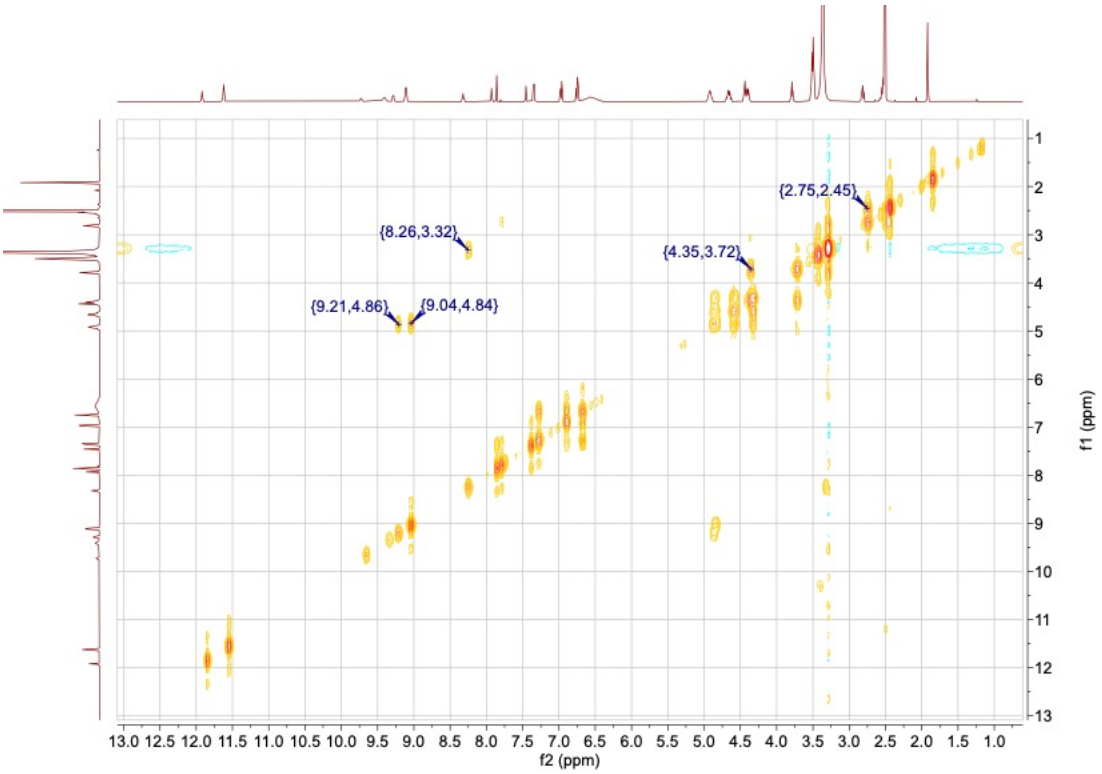

^{1}H-^{13}C HSQC

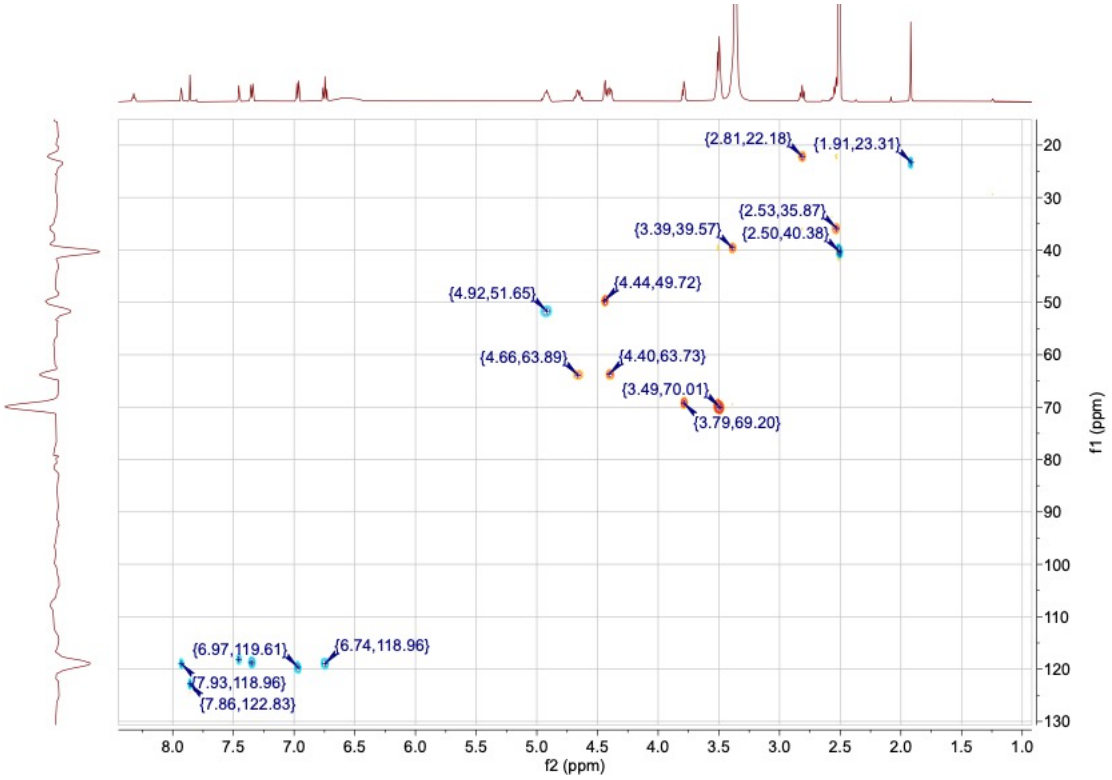

^{1}H-^{13}C HMBC

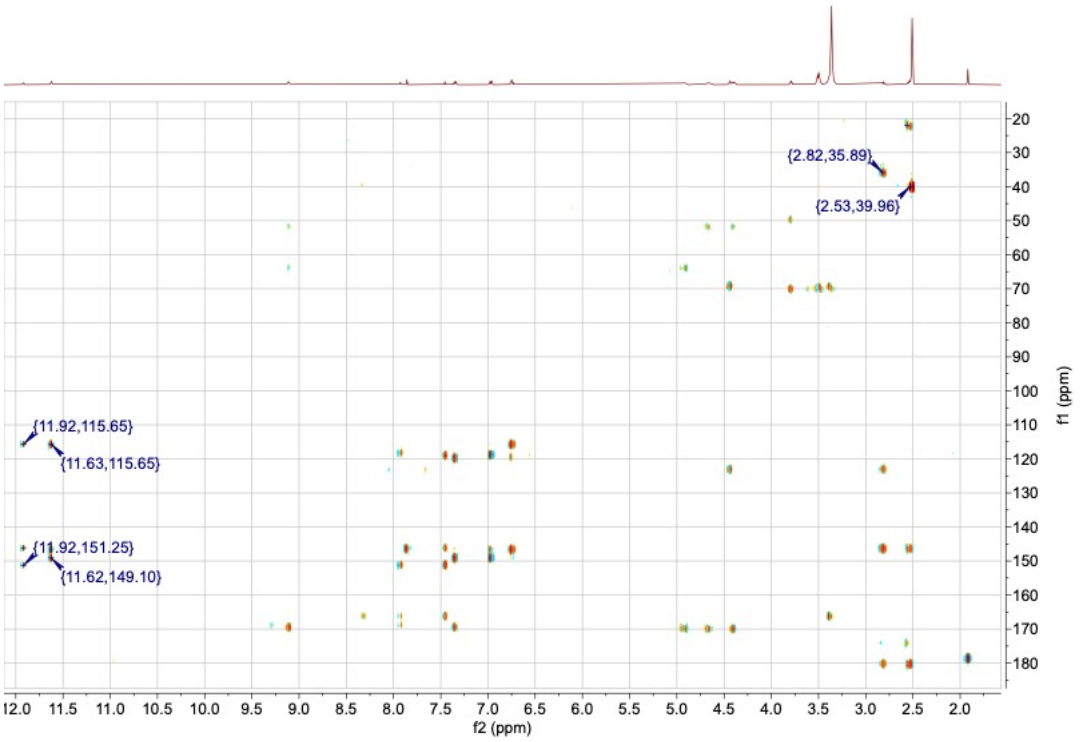

^{1}H-^{195}Pt HMQC

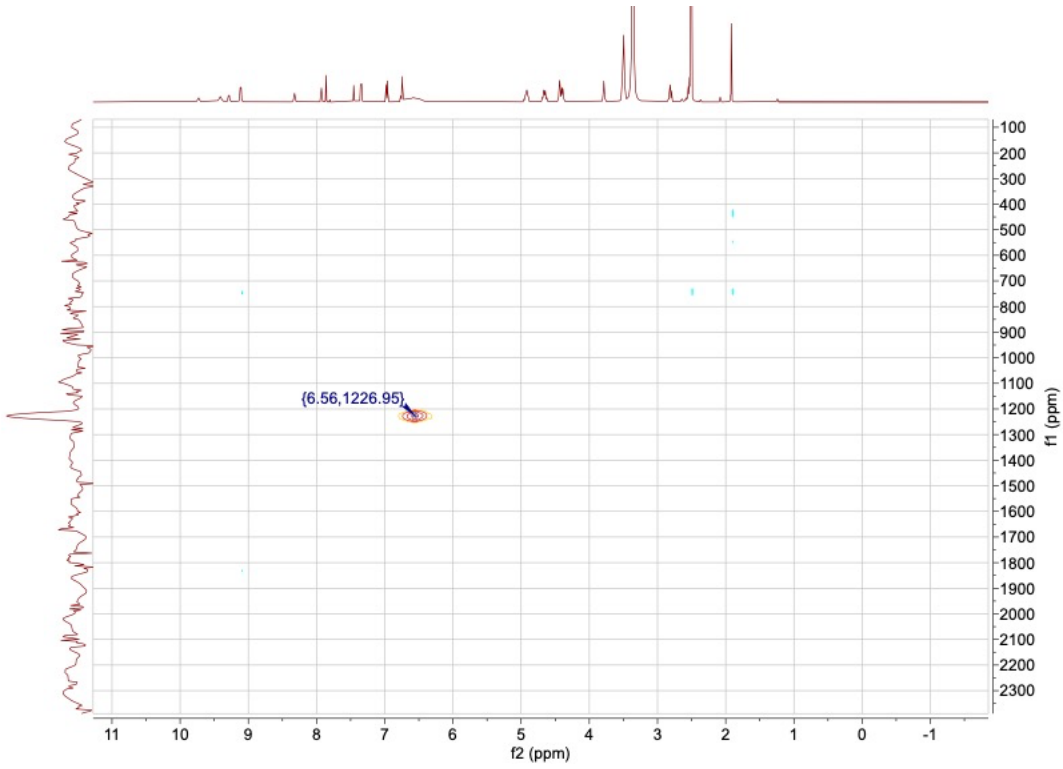

References

1. Zheng, T.; Nolan, E. M., Enterobactin-mediated delivery of *β*-lactam antibiotics enhances antibacterial activity against pathogenic *Escherichia coli*. *J. Am. Chem. Soc.* **2014,** *136*, 9677-9691.
2. Zheng, T.; Bullock, J. L.; Nolan, E. M., Siderophore-mediated cargo delivery to the cytoplasm of *Escherichia coli* and *Pseudomonas aeruginosa*: syntheses of monofunctionalized enterobactin scaffolds and evaluation of enterobactin–cargo conjugate uptake. *J. Am. Chem. Soc.* **2012,** *134*, 18388-18400.
3. Ramirez, R. J.; Karamanukyan, L.; Ortiz, S.; Gutierrez, C. G., A much improved synthesis of the siderophore enterobactin. *Tetrahedron lett.* **1997,** *38*, 749-752.
4. Ravera, M.; Gabano, E.; Tinello, S.; Zanellato, I.; Osella, D., May glutamine addiction drive the delivery of antitumor cisplatin-based Pt(IV) prodrugs? *J. Inorg. Biochem.* **2017,** *167*, 27-35.
5. Zhang, J. Z.; Bonnitcha, P.; Wexselblatt, E.; Klein, A. V.; Najajreh, Y.; Gibson, D.; Hambley, T. W., Facile preparation of mono-, di- and mixed-carboxylato platinum(IV) complexes for versatile anticancer prodrug design. *Chemistry* **2013,** *19*, 1672-1676.
6. Scarrow, R. C.; Ecker, D. J.; Ng, C.; Liu, S.; Raymond, K. N., Iron(III) coordination chemistry of linear dihydroxyserine compounds derived from enterobactin. *Inorg. Chem.* **1991,** *30*, 900-906.
7. Johnstone, T. C.; Alexander, S. M.; Lin, W.; Lippard, S. J., Effects of monofunctional platinum agents on bacterial growth: a retrospective study. *J. Am. Chem. Soc.* **2014,** *136*, 116-118.
8. Neumann, W.; Sassone-Corsi, M.; Raffatellu, M.; Nolan, E. M., Esterase-catalyzed siderophore hydrolysis activates an enterobactin-ciprofloxacin conjugate and confers targeted antibacterial activity. *J. Am. Chem. Soc.* **2018,** *140*, 5193-5201.
9. Chairatana, P.; Zheng, T.; Nolan, E. M., Targeting virulence: salmochelin modification tunes the antibacterial activity spectrum of β-lactams for pathogen-selective killing of *Escherichia coli*. *Chem. Sci.* **2015,** *6*, 4458-4471.
10. Blango, M. G.; Ott, E. M.; Erman, A.; Veranic, P.; Mulvey, M. A., Forced resurgence and targeting of intracellular uropathogenic *Escherichia coli* reservoirs. *PLoS One* **2014,** *9*, e93327.
11. Johnstone, T. C.; Suntharalingam, K.; Lippard, S. J., The next generation of platinum drugs: targeted Pt(II) agents, nanoparticle delivery, and Pt(IV) prodrugs. *Chem. Rev.* **2016,** *116*, 3436-3486.
12. Wilson, J. J.; Lippard, S. J., Synthetic methods for the preparation of platinum anticancer complexes. *Chem. Rev.* **2014,** *114*, 4470-4495.
13. Wexselblatt, E.; Yavin, E.; Gibson, D., Platinum(IV) prodrugs with haloacetato ligands in the axial positions can undergo hydrolysis under biologically relevant conditions. *Angew. Chem. Int. Ed.* **2013,** *52*, 6059-6062.
14. Zheng, T.; Nolan, E. M., Evaluation of (acyloxy)alkyl ester linkers for antibiotic release from siderophore-antibiotic conjugates. *Bioorg. Med. Chem. Lett.* **2015,** *25* (21), 4987-4991.
15. Frank, R. A. W.; Leeper, F. J.; Luisi, B. F., Structure, mechanism and catalytic duality of thiamine-dependent enzymes. *Cell. Mol. Life Sci.* **2007,** *64*, 892-905.

16. Baba, T.; Ara, T.; Hasegawa, M.; Takai, Y.; Okumura, Y.; Baba, M.; Datsenko, K. A.; Tomita, M.; Wanner, B. L.; Mori, H., Construction of *Escherichia coli* K-12 in-frame, single-gene knockout mutants: the Keio collection. *Mol. Syst. Biol.* **2006,** *2*, 2006.0008.